The Canadian Mineralogist
Vol. 41, pp. 1027-1047 (2003)

OSCILLATORY EPITACTIC-GROWTH ZONING IN BIOTITE AND MUSCOVITE FROM THE LAKE LEWIS LEUCOGRANITE, SOUTH MOUNTAIN BATHOLITH, NOVA SCOTIA, CANADA

D. BARRIE CLARKE§ AND PATRICK A. BOGUTYN

Department of Earth Sciences, Dalhousie University, Halifax, Nova Scotia B3H 3J5, Canada

ABSTRACT

The Lake Lewis leucogranite, with high levels of Rb, Li, B, Nb, Ta, Sn, U, Th and F, is a strongly fractionated pluton in the South Mountain Batholith, Nova Scotia. Its main minerals are quartz + albite + K-feldspar ± topaz + four fluorine-rich mica phases: Bt_1, an early magmatic biotite as inclusions in quartz, Bt_2, the main pleochroic dark mica, Ms_{ss}, the main white mica, and IMP, a weakly pleochroic intermediate mica phase. The IMP normally occurs as straight, sharp, optically continuous, oscillatory, variably heterogeneous, epitactic overgrowths on Bt_2 and Ms_{ss}. All micas are texturally primary magmatic. The major-element compositions of IMP are intermediate between Ms_{ss} and Bt_2. The average trace-element compositions of the Lake Lewis Ms_{ss} (n = 24) and IMP (n = 15) zones by LAM–ICP–MS are (in ppm): Sc 18.6, 20.3; V 3.6, 9.3; Zr 3.2, 1.2; Hf 0.32, 0.20; Nb 167, 167; Ta 13.7, 21.2; Rb 2369, 3090; Cs 62, 433; and Ba 11, 31, respectively. Oscillatory zoning involving Bt_2–IMP and Ms_{ss}–IMP suggests crystallization under oscillating T–P–X conditions. Repeated build-up and release of H_2O pressure in the magma chamber might explain the oscillatory epitactic-growth zoning in these micas: the Bt_2 and Ms_{ss} zones crystallize from the silicate melt when P is lithostatic and $a(H_2O)$ is less than 1, and the IMP zones crystallize from the silicate melt with trace-element populations modified by the evolution of a fluid phase, when P exceeds lithostatic pressure and $a(H_2O)$ is equal to 1. The heterogeneity of IMP may be related to subsolidus breakdown or exsolution. Epitactically zoned micas of the Lake Lewis leucogranite may act as pressure gauges on the hydraulic pump responsible for the formation of hydrothermal alteration, aplite – pegmatite – greisen, mineral deposits, cataclasis, and even eruption of the magma chamber.

Keywords: biotite, muscovite, epitactic growth, fluid phase, overpressure, fluorine, exsolution, eruption, Lake Lewis pluton, Nova Scotia.

SOMMAIRE

Le pluton leucogranitique dit de Lake Lewis, à teneurs élevées en Rb, Li, B, Nb, Ta, Sn, U, Th et F, est un membre fortement évolué du batholithe de South Mountain, en Nouvelle-Écosse. Les minéraux principaux sont quartz + albite + feldspath potassique ± topaze + quatre membres du groupe des micas: Bt_1, une biotite magmatique précoce, piégée dans le quartz, Bt_2, le mica sombre pléochroïque principal, Ms_{ss}, le mica blanc principal, et PMI, phase micacée intermédiaire à faible pléochroïsme. Le mica PMI se présente normalement en surcroissance rectiligne, bien définie, optiquement continue, à comportement oscillatoire, quelque peu hétérogène, et épitactique sur Bt_2 et Ms_{ss}. Tous les micas semblent primaires (magmatiques) d'après leur texture. La composition de PMI, en termes d'éléments majeurs, se situe entre Ms_{ss} et Bt_2. En termes d'éléments-traces, la muscovite Ms_{ss} (n = 24) et le mica PMI (n = 15), analysés par LAM–ICP–MS, contiennent (en ppm): Sc 18.6, 20.3; V 3.6, 9.3; Zr 3.2, 1.2; Hf 0.32, 0.20; Nb 167, 167; Ta 13.7, 21.2; Rb 2369, 3090; Cs 62, 433; et Ba 11, 31, respectivement. Des oscillations impliquant Bt_2–IMP et Ms_{ss}–IMP témoigneraient d'une cristallisation en présence d'oscillations des variables T–P–X. Des montées et évacuations répétées de la pression de H_2O dans la chambre magmatique pourraient expliquer les oscillations en croissance épitactique dans ces micas: les zones Bt_2 et Ms_{ss} auraient cristallisé à partir du magma à un point où la pression était lithostatique et où $a(H_2O)$ était inférieur à 1, tandis que les zones à mica PMI auraient cristallisé à partir d'un magma dont les populations d'éléments-traces avaient été modifiées suite à l'exsolution d'une phase gazeuse, lors d'une période où la pression dépassait la pression lithostatique, et où la valeur de $a(H_2O)$ était égale à 1. L'hétérogénéité du mica PMI pourrait bien résulter d'une déstabilisation subsolidus ou d'une exsolution. Les micas à zones de croissance épitactiques oscillatoires du leucogranite de Lake Lewis agiraient en quelque sorte de manomètre sur la pompe hydraulique responsable de l'altération hydrothermale, de l'association aplite – pegmatite – greisen, des gîtes minéraux, de la cataclase, et même de l'éruption de la chambre magmatique.

(Traduit par la Rédaction)

Mots-clés: biotite, muscovite, croissance épitactique, phase fluide, surpression, fluor, exsolution, éruption, pluton de Lake Lewis, Nouvelle-Écosse.

§ *E-mail address*: clarke@dal.ca

INTRODUCTION

The South Mountain Batholith of southwestern Nova Scotia is a large, post-tectonic, late Devonian (≥372 Ma), highly fractionated, peraluminous granitic complex, with rock types ranging from biotite granodiorite to muscovite–topaz leucogranite (Clarke & Muecke 1985, Tate & Clarke 1997, MacDonald 2001). The chemically most evolved rocks are the rare (<1%) late leucogranites occurring as small, discrete, and texturally variable bodies in the interior of the batholith (Clarke *et al.* 1993). These leucogranites consist primarily of quartz + sodic plagioclase + K-feldspar + muscovite ± biotite ± andalusite ± topaz.

Our purpose is to use the major- and trace-element compositions of chemically zoned biotite and muscovite from the Lake Lewis leucogranite in the South Mountain Batholith to test their primary magmatic character, to deduce the conditions under which they crystallized, and to consider the wider implications of these zoned flakes of mica.

BACKGROUND INFORMATION

The Lake Lewis leucogranite

The Lake Lewis leucogranite (Fig. 1) is a small (4–5 km^2), white to cream-colored, fine- to medium-grained, generally equigranular but locally porphyritic pluton intruding the New Ross leucomonzogranite (Ham 1991). Modally, the pluton contains >10% muscovite and <3% biotite. Geochemically, the Lake Lewis leucogranite is among the most evolved plutons in the South Mountain Batholith, with strong enrichment in incompatible elements (Rb, Li, B, F, Nb, Ta, Sn, U, Th) and H_2O, and strong depletion in compatible elements (Ba, Sr, Ti, Zr, Hf) (Clarke *et al.* 1993). Minor pegmatite and aplite dykes and quartz-vein stockworks are common within the pluton. Although the pluton has no regional tectonic fabric, many rocks show strong cataclasis. Molybdenum, uranium, and fluorine mineralization occurs within the Lake Lewis leucogranite as disseminations in the groundmass, along hematite-lined fractures and shear planes, and in minor pegmatites (Ham 1991).

Chemical zoning in minerals

Most rock-forming minerals in granites belong to solid-solution series, and thus can show chemical zonation with, or without, any optical manifestation of the compositional variation (*e.g.*, K-feldspar and plagioclase, respectively). Biotite and muscovite also may show chemical variation within single grains, normally without any detectable change in optical properties. In all such cases, compositional zoning in minerals records rates of crystallization that are greater than rates of chemical equilibration. The chemical disequilibrium may be manifest as continuous normal or reverse compositional zoning, or as continuous or discontinuous oscillatory zoning. Ding (1995) documented a variety of zoned Al–Fe–Mg silicate minerals, including biotite, muscovite, cordierite, andalusite, and garnet, from the South Mountain Batholith.

White mica (muscovite) is arguably the most problematic rock-forming mineral in granites. The P–T stability curve of end-member muscovite intersects the minimum melting curve of granite at approximately 2.5 kbar and 625ºC (Chatterjee & Johannes 1974). If the thermal stability of white mica increases with increasing Fe and F content (Monier & Robert 1986a), and if the minimum melting curve of granite decreases with high fluorine content (Weidner & Martin 1987), the stability field of primary magmatic white mica also expands considerably. Thus, muscovite may crystallize directly from a silicate melt of granitic composition at pressures above ~1 kbar (primary, magmatic), or it may crystallize in the solid state at any pressure or temperature below the stability curve of muscovite (secondary, subsolidus). Although the genesis of muscovite has been studied in many plutons (Miller *et al.* 1981, Speer 1984, Zen 1988), no consensus concerning the diagnostic textural criteria (size, shape, relation to other minerals), or chemical criteria (*e.g.*, TiO_2, Na_2O/K_2O, FeO + MgO, compositions in equilibrium with other phases, zoning) for an unambiguous primary magmatic or secondary origin have yet emerged. Optically detectable oscillatory zoning in muscovite from the Leinster granite (Roycroft 1989, 1991) has provided the most convincing textural evidence for a primary magmatic origin, although Ortoleva (1994) has claimed that such zoning can develop in many other environments of crystallization.

Chemical zoning in end-member dioctahedral muscovite [$K_2Al_4Si_6Al_2O_{20}(OH,F)_4$] can follow three substitutional schemes involving cations: (i) toward celadonite: $2^{IV}Al \leftrightarrow {}^{VI}Fe + {}^{IV}Si$ (Tschermak substitution), (ii) toward annite: $4^{VI}Al + 2\,{}^{VI}\square \leftrightarrow 6^{VI}Fe$ (biotite substitution), and (iii) toward siderophyllite: $2^{VI}Al + 2^{VI}\square + 2^{IV}Si \leftrightarrow 4^{VI}Fe + 2^{IV}Al$, where ${}^{VI}\square$ represents a vacant octahedral site. Naturally occurring white micas in granitic rocks appear to have compositions that involve some combination of these substitutions (Monier & Robert 1986a).

Ham & Kontak (1988) examined micas from the South Mountain Batholith and could find no systematic correlation between the various textural varieties and their compositions. They reported that only a small modal percentage of the white micas seems to be primary on textural grounds, but that chemically, a large proportion appears to have formed as an integral part of the magmatic evolution because of the correlation between trace-element contents of the mica and the compositions of the bulk rocks containing them.

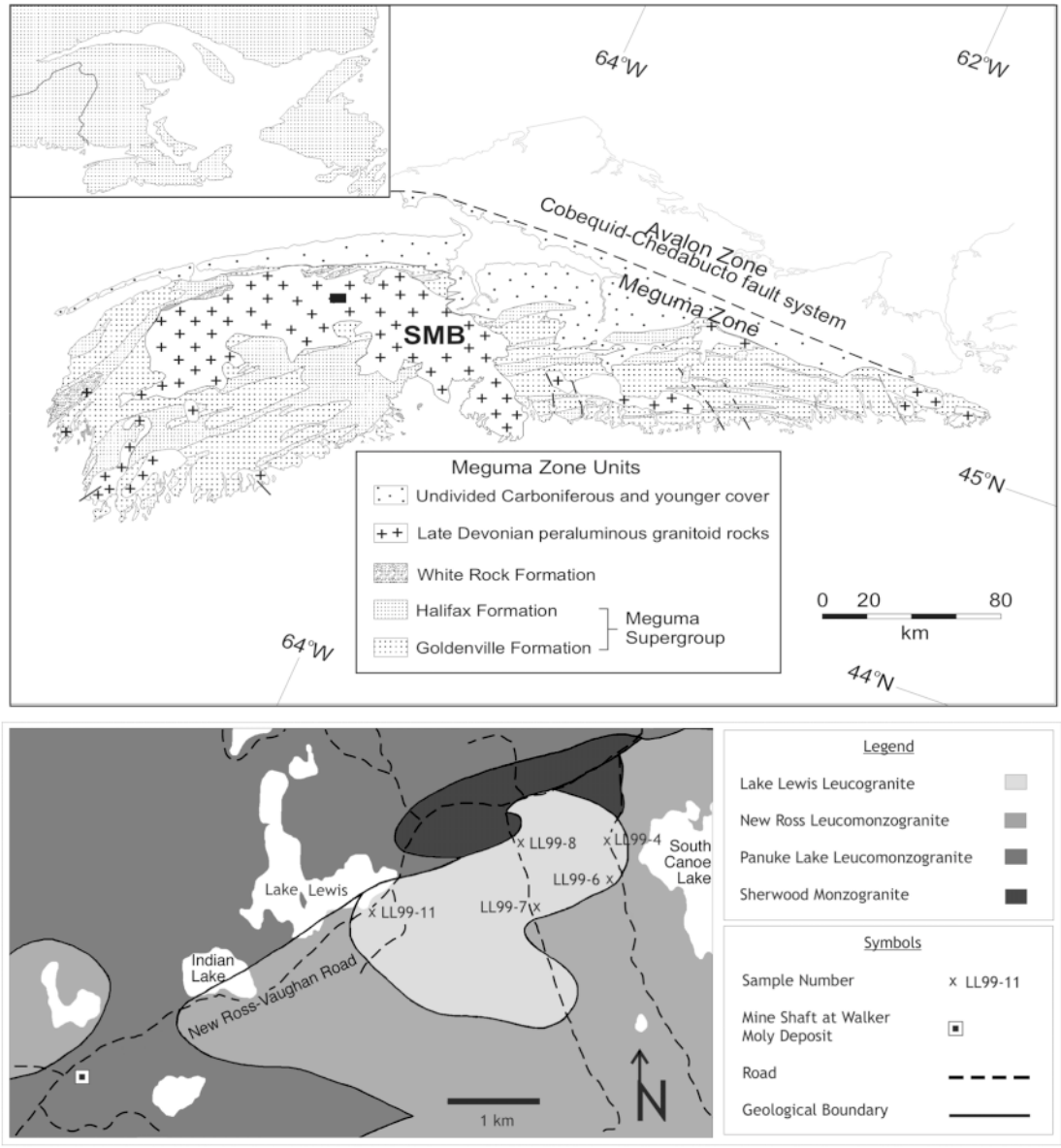

FIG. 1. General location map of the South Mountain Batholith in southwestern Nova Scotia (above), showing the position of the Lake Lewis leucogranite (black rectangle). Geological map of the Lake Lewis leucogranite (simplified after Ham 1991), showing sample locations and position of the Walker Mo–Cu mineral deposit.

METHODS

We collected leucogranite samples from three traverses through the Lake Lewis leucogranite (Fig. 1), and used transmitted light microscopy on standard thin sections to assessment of textural features in relation to the origin of the white micas (Bogutyn 2001). We also used polished thin sections to analyze for major elements with a JEOL 8200 electron microprobe X-ray microanalyzer in the Dalhousie Regional Electron Microprobe Laboratory. The instrument is equipped with five wavelength-dispersion spectrometers. We operated

it at 15 kV, 15 nA, 10 μm spot size, and 40-second counting times, using the following geological standards: sanidine for Si, Al, K; Kakanui kaersutite for Ti, Mg, Ca; almandine 12442 for Fe; jadeite for Na; MnO_2 for Mn; and fluorapatite for F. We took particular care with backgrounds in the vicinity of the Fe$L\alpha_1$–F$K\alpha_1$ interference region to obtain reliable concentrations of F. All reported compositions are the averages of not less than ten spot analyses, and considerably more randomly selected spot analyses and tracks in the case of the heterogeneous intermediate mica phase (see below).

We lightly crushed and hand-picked the grains of white mica to search for zoned crystals. The separated crystals showing zoning were analyzed for trace elements by laser-ablation microprobe ICP–MS (LAM–ICP–MS) at the University of Victoria. A Merchantek UV laser-ablation microprobe (LAM) coupled with the VG PQIIS is capable of determining concentrations of a large suite of trace elements in various solids with good precision and accuracy. The method is best suited to the determination of elements heavier than and including Rb, especially the lithophile suite (Sr, Y, Zr, Nb, Ba, REE, Hf, Ta, Th, and U) (Longerich *et al.* 1996). Data were acquired in the peak-jumping mode, with a dwell time of 10 ms. Background levels for each element are obtained by acquiring data for a gas blank for approximately 40 seconds prior to laser sampling. Calibration and quantification of the analysis utilize both external and internal calibrations. Drift, matrix effect, changes in laser-sampling yield, and transport efficiency during the analysis are corrected for by using naturally occurring internal standards. Therefore, the accurate known concentration of at least one analytically suitable major element (*e.g.*, Ca, Mg, or Si) homogeneously distributed in the sample is required.

Typical limits of detection vary from a few ppm to a few ppb depending upon elements determined and operating conditions. Spot size and laser power are two important parameters affecting the limits of detection. Spot sizes of about 50 μm and laser energy of less than 3 mJ per pulse are normally used for routine analysis. However, spot sizes as small as 5 μm can be achieved by computer-controlled beam aperture if the grain size is very small or a high-resolution sampling is required.

Results: General Petrographic Observations

All samples of the Lake Lewis leucogranite have similar modal percentages of quartz (25 ± 5%), K-feldspar (25 ± 5%), plagioclase (35 ± 5%), white mica (15 ± 5%) and biotite (1–3%). Some samples also contain small amounts of accessory minerals such as topaz, fluorite, and zircon. The topaz grains are subhedral in shape and may contain small inclusions of biotite and overgrowths of mica. Except for rare phenocrysts and pegmatitic portions, most of the Lake Lewis leucogranite is medium grained and equigranular. Secondary alteration, as manifest in flakes of white mica in plagioclase, kaolinite in K-feldspar, and domains of chlorite in biotite, is variable but minor.

Textural Relations of the Micas

Biotite

Biotite forms a relatively minor constituent in most rocks of the pluton. It may occur as small, euhedral inclusions in quartz or feldspar (Bt_1). It may also occur as euhedral to anhedral grains (Bt_2), commonly mantled by a weakly pleochroic brown mica in optical continuity. The contact between Bt_2 and its mantles may be straight and optically sharp or irregular and optically diffuse (Fig. 2). Although Bt_1 and Bt_2 occur in the same rock, they have different compositions (see below).

Muscovite

Muscovite occurs as colorless, coarse-grained (0.5–4 mm), euhedral to anhedral crystals, dimensionally compatible with other silicate minerals, with generally straight, optically sharp boundaries against coexisting minerals, including optically continuous mantles of a weakly pleochroic brown mica. Visual inspection of relatively large, single, hand-picked grains of this muscovite, using Roycroft's (1989, 1991) thick section (~0.3 mm) method, reveals that several grains have well-defined alternating compositional bands. Figure 3 shows two thick grains of muscovite (LL99–6–1, LL99–8–1), with compositional zoning involving repeated layers of colorless mica and weakly pleochroic light brown mica in plane-polarized light. The contacts between the two types of mica are straight and sharp. Because the alternating colorless and light brown zones are in optical and crystallographic continuity, we refer to them hereafter as oscillatory epitactic zones.

Intermediate mica phase (*IMP*)

IMP (intermediate mica phase) refers to the weakly pleochroic pale brown mica that occurs as optically continuous mantles on biotite (Fig. 2) and muscovite (Figs. 3, 4). The optic axial planes of these mantling micas are coincident with their biotite or muscovite cores, and thus all core and mantle domains extinguish optically at the same position. Whereas the biotite and muscovite appear to be compositionally homogeneous, the IMP appears to be variably heterogeneous in backscattered electron images.

Chemical Compositions of the Micas

The major elements

Table 1 contains the average major-element compositions of the four mica phases in several widely separated samples from the Lake Lewis leucogranites, and

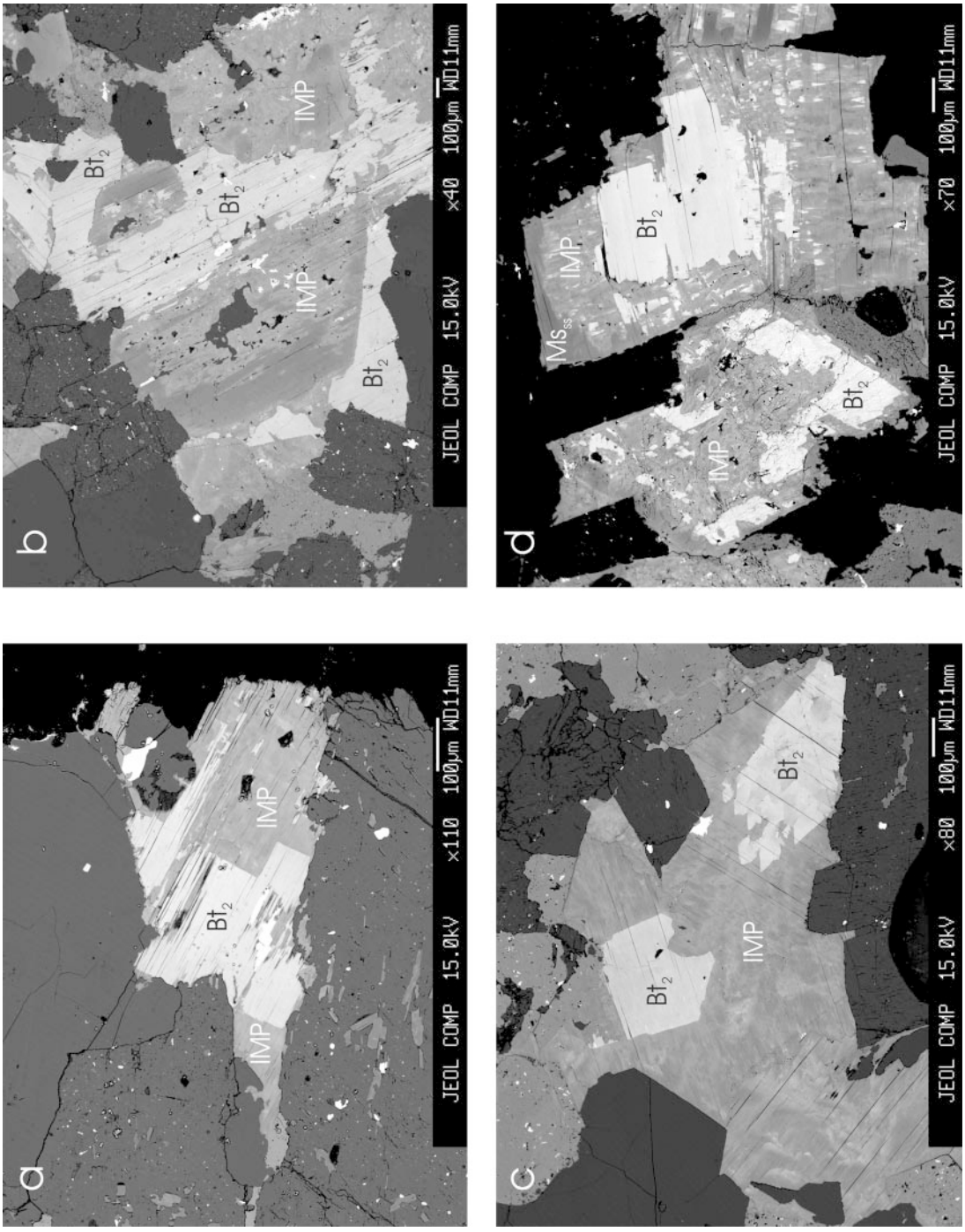

FIG. 2. Back-scattered electron images showing textural relations of biotite grains in sample LL99–7 of the Lake Lewis leucogranite. (a) Biotite core (Bt_2) with straight, sharp grain-boundaries against an intermediate mica phase (IMP). (b) Irregular core in biotite on which has nucleated a euhedral overgrowth of the intermediate phase, followed by an outer rim of biotite. (c) Subhedral biotite overgrown by extensive rim of the intermediate phase. (d) Grain on left shows a sequence from (biotite?) to intermediate phase to biotite to intermediate phase. Grain on right shows the sequence biotite – intermediate phase – muscovite. All mica domains are in optical continuity.

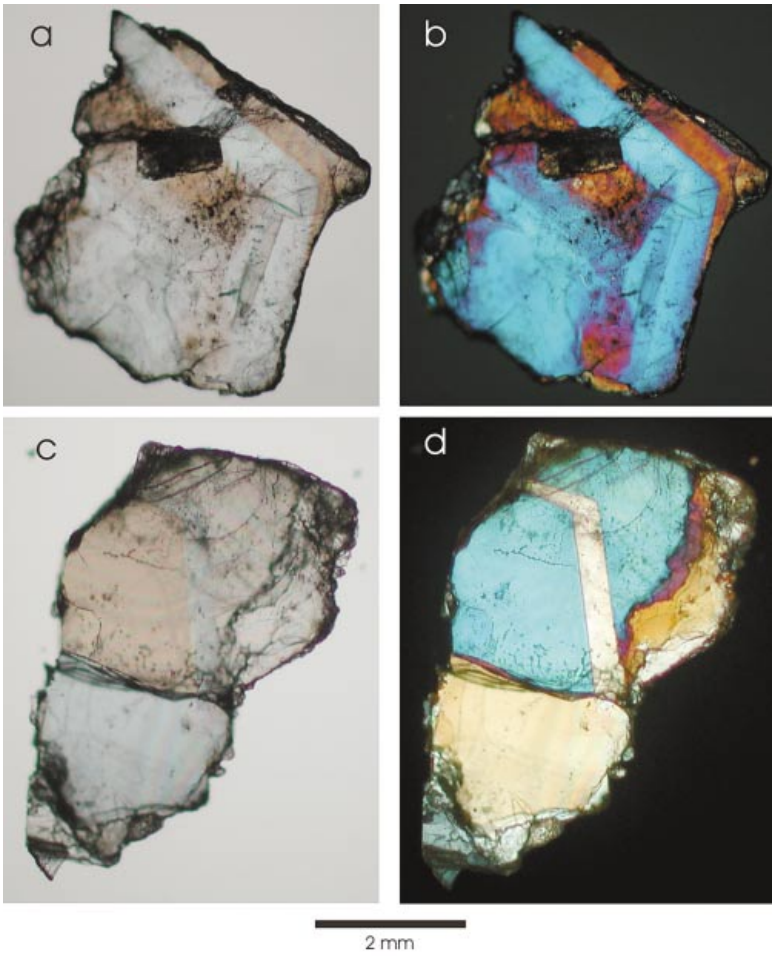

FIG. 3. Textural relations in white mica in thick cleavage fragments. (a–b) Grain LL99–6–1 in plane-polarized light and crossed nicols, respectively. (c–d) Grain LL99–8–1 in plane-polarized light and crossed nicols, respectively. The colorless mica in plane-polarized light is muscovite (Ms_{ss}). The pale brown mica in plane-polarized light is the intermediate mica phase (IMP). All mica zones are in optical continuity.

Figure 5 shows these compositions in relation to each other and also in relation to end-member mica compositions. In general terms, Bt_1 and Bt_2 have compositions that are intermediate between stoichiometric trioctahedral and stoichiometric dioctahedral micas. Bt_1 has a greater octahedral-site occupancy than Bt_2, and Bt_1 contains less fluorine than Bt_2 at the same stage of magmatic evolution, as measured by Fe/(Fe + Mg) (Fig. 6). The optically identified muscovite (Ms_{ss}), with FeO contents of 3.29–7.62 wt.%, combines the Tschermak substitution toward celadonite, and biotite substitution toward phlogopite–annite. Although the muscovite has a high FeO content, it has the lowest concentrations of fluorine (2.19–3.40 wt. %) of the four mica phases present in these rocks. Finally, the IMP is also muscovite (Rieder *et al.* 1998), intermediate in composition between Bt_2 and Ms_{ss}, although lying much closer to the Ms_{ss} composition (Figs. 5, 6). The back-scattered electron images (Figs. 2, 4) clearly show the heterogeneous nature of the IMP. Spot analyses in the dark and light areas yield mica compositions with low and high contents of Fe, respectively.

Calculation of lithium contents for these micas, using equation *tri1* [$Li_2O = (0.289*SiO_2) – 9.658$] for the "trioctahedral" Bt_1 and Bt_2, and equation *di1* [$Li_2O = 0.3935F^{1.326}$] for the "dioctahedral" Ms_{ss} (Tischendorf *et al.* 1997), has the general effect of filling the vacant octahedral sites with Li. According to a modified ver-

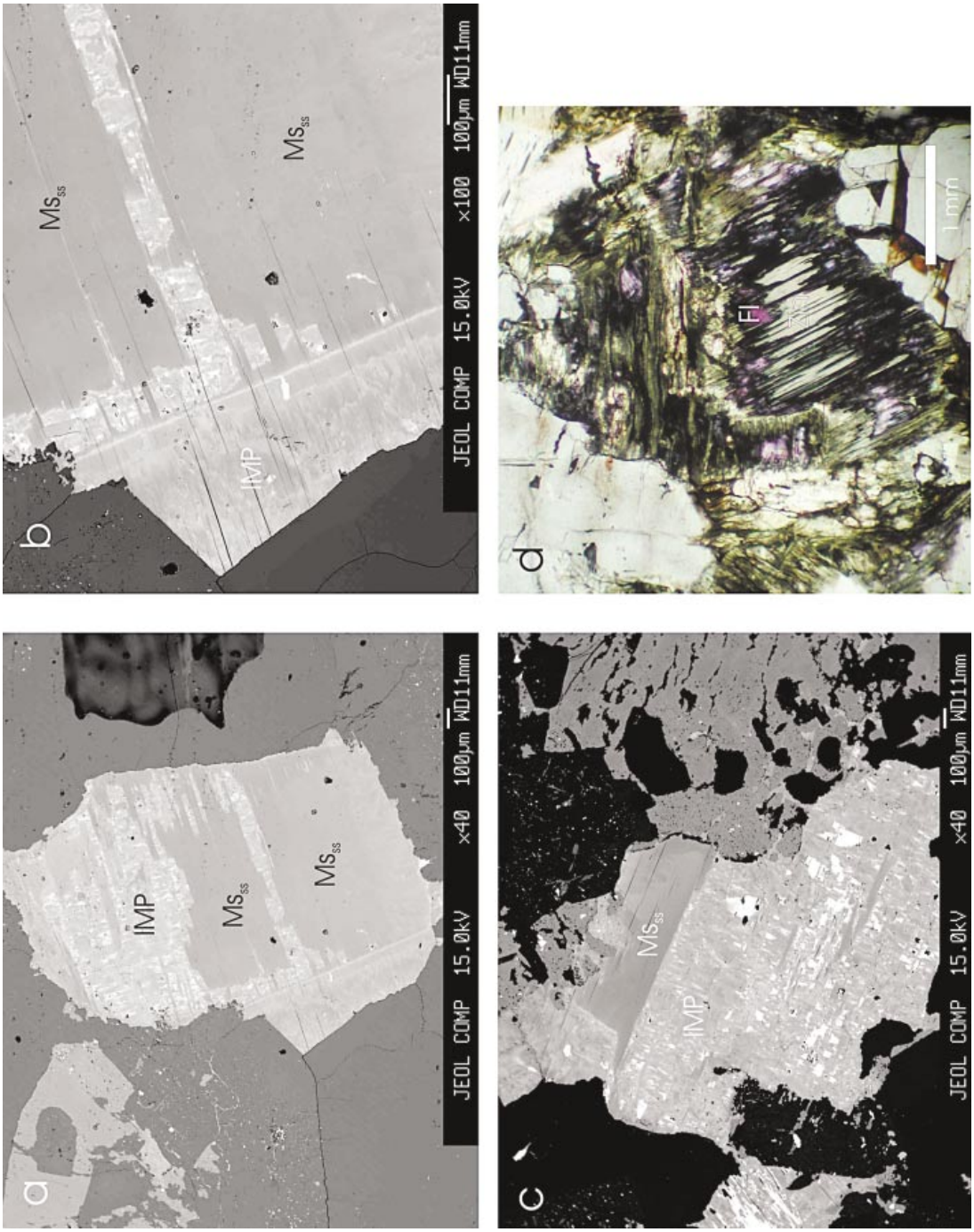

FIG. 4. Textural relations of the white mica in thin section. (a) Muscovite with overgrowth of intermediate phase mica. (b) Detail of (a) showing the sharp but irregular grain-boundaries between muscovite and the intermediate mica phase (IMP), in places suggesting some corrosion of the muscovite before crystallization of the IMP. Note also the chemical heterogeneity of IMP. (c) IMP with an overgrowth of muscovite. Previous three photographs are back-scattered electron images. All mica zones are in optical continuity. (d) Fractured and altered muscovite from the Walker Moly deposit in plane-polarized light. Fluorite (Fl) has crystallized in the muscovite cleavages, and the original muscovite has altered to a zinnwaldite series (Zin) mica (Bogutyn 2001). The same texture and alteration occur in micas from cataclastic rocks in the Lake Lewis leucogranite.

TABLE 1. CHEMICAL COMPOSITION§ OF MICAS FROM THE LAKE LEWIS LEUCOGRANITE, NOVA SCOTIA

Sample	M79	99-6	99-7	99-8	99-4	99-6	99-7	99-8	99-4	99-6	99-7	99-8	99-11	99-4	99-6	99-7	99-8	99-11
Mineral	Bt	Bt1	Bt1	Bt1	Bt2	Bt2	Bt2	Bt2	IMP	IMP	IMP	IMP	IMP	Ms	Ms	Ms	Ms	Ms
SiO_2 wt.%	35.12	37.53	37.68	37.51	40.66	40.15	40.04	39.98	44.26	45.17	44.97	44.73	45.37	45.66	46.26	45.30	45.31	45.78
TiO_2	3.84	2.26	1.29	2.36	0.84	1.36	1.06	0.92	0.48	0.49	0.53	0.51	0.34	0.38	0.24	0.29	0.18	0.16
Al_2O_3	18.77	21.31	22.35	21.07	24.13	22.89	23.74	23.56	27.73	28.59	28.66	28.52	30.85	27.14	31.41	30.32	30.76	33.63
FeO	21.17	21.86	20.68	21.19	16.04	17.37	17.12	16.68	9.00	7.43	7.88	7.84	5.95	7.62	4.25	5.64	5.36	3.29
MnO	0.58	0.33	0.40	0.30	0.32	0.32	0.42	0.31	0.15	0.16	0.20	0.16	0.16	0.10	0.09	0.12	0.12	0.06
MgO	5.64	0.94	0.98	0.76	0.54	0.76	0.81	0.74	0.53	0.70	0.69	0.62	0.45	0.44	0.61	0.67	0.64	0.42
Li_2O*	0.49	1.19	1.23	1.18	2.09	1.94	1.91	1.90	2.31	2.02	2.10	2.27	1.65	1.99	1.47	1.66	1.98	1.11
CaO	0.01	0.00	0.01	0.01	0.00	0.00	0.01	0.02	0.00	0.00	0.00	0.01	0.00	0.02	0.00	0.00	0.01	0.00
Na_2O	0.16	0.22	0.29	0.23	0.29	0.20	0.34	0.28	0.35	0.46	0.37	0.41	0.57	0.28	0.71	0.69	0.74	0.86
K_2O	9.68	10.09	10.08	10.05	10.34	10.56	9.94	9.87	10.85	11.00	10.76	10.76	10.72	10.66	10.96	10.70	10.54	10.24
H_2O**	3.59	2.06	2.02	1.92	1.81	1.84	1.97	1.82	2.53	2.76	2.70	2.59	3.03	2.70	3.18	2.99	2.83	3.45
F	0.63	4.00	4.07	4.22	4.85	4.73	4.47	4.70	3.79	3.43	3.53	3.75	2.95	3.40	2.70	2.97	3.38	2.19
Total	99.68	101.79	101.07	100.79	101.92	102.12	101.83	100.80	101.99	102.20	102.40	102.17	102.03	100.40	101.87	101.35	101.84	101.21
less F=O	0.26	1.69	1.71	1.78	2.04	1.99	1.58	1.69	1.51	1.44	1.06	1.42	1.24	1.43	1.14	0.97	1.32	0.92
Total	99.42	100.11	99.36	99.02	99.88	100.13	100.25	99.12	100.48	100.76	101.34	100.76	100.78	98.97	100.74	100.38	100.52	100.29
Si *apfu*	5.399	5.689	5.713	5.733	5.930	5.904	5.870	5.914	6.137	6.189	6.159	6.146	6.150	6.353	6.221	6.179	6.142	6.128
^{IV}Al	2.601	2.311	2.287	2.267	2.070	2.096	2.130	2.086	1.863	1.811	1.841	1.854	1.850	1.647	1.779	1.821	1.858	1.872
^{VI}Al	0.801	1.495	1.709	1.529	2.079	1.872	1.972	2.022	2.670	2.806	2.785	2.765	3.078	2.804	3.200	3.053	3.057	3.433
Ti	0.444	0.258	0.147	0.271	0.092	0.150	0.117	0.103	0.050	0.050	0.054	0.052	0.034	0.040	0.024	0.029	0.019	0.017
Fe^{2+}	2.722	2.770	2.623	2.709	1.956	2.136	2.100	2.064	1.044	0.851	0.903	0.901	0.674	0.886	0.478	0.644	0.607	0.369
Mn	0.075	0.042	0.051	0.039	0.040	0.039	0.052	0.039	0.018	0.018	0.024	0.019	0.018	0.012	0.010	0.014	0.013	0.007
Mg	1.293	0.213	0.221	0.173	0.118	0.167	0.176	0.163	0.110	0.143	0.140	0.127	0.091	0.092	0.122	0.136	0.128	0.085
Li	0.303	0.725	0.751	0.727	1.228	1.150	1.128	1.128	1.286	1.111	1.156	1.255	0.900	1.116	0.793	0.912	1.081	0.600
Ca	0.002	0.001	0.001	0.002	0.000	0.001	0.001	0.003	0.000	0.000	0.000	0.002	0.000	0.002	0.000	0.000	0.001	0.000
K	1.898	1.951	1.949	1.959	1.925	1.981	1.858	1.863	1.919	1.923	1.881	1.887	1.853	1.892	1.881	1.862	1.823	1.749
Na	0.048	0.066	0.086	0.068	0.081	0.056	0.097	0.081	0.094	0.122	0.097	0.109	0.150	0.076	0.185	0.183	0.194	0.224
OH	3.685	2.085	2.045	1.959	1.763	1.807	1.928	1.797	2.342	2.525	2.469	2.376	2.742	2.508	2.855	2.723	2.562	3.083
Total	0.304	1.920	1.952	2.041	2.239	2.199	2.073	2.200	1.664	1.486	1.531	1.630	1.265	1.496	1.147	1.279	1.451	0.928
Sum cations	15.586	15.519	15.537	15.475	15.519	15.553	15.503	15.468	15.192	15.025	15.041	15.115	14.800	14.921	14.693	14.832	14.924	14.484

* Li values calculated using the equations of Tischendorf *et al.* (1997). ** H_2O values calculated assuming the OH–F site is full and amount of Cl is negligible. Proportion of cations based on 24(O,OH,F), expressed in cations per formula unit (*apfu*). IMP: intermediate mica phase, Ms: muscovite, Bt: biotite. § Electron-microprobe data.

sion of the "feal–mgli" classification (H.-J. Förster, pers. commun.), Bt_1 is siderophyllite, Bt_2 is siderophyllite bordering on lithian siderophyllite, Ms_{ss} is ferroan muscovite, and IMP is lithian–ferroan muscovite.

The Trace Elements

Table 2 contains the trace-element concentrations in Ms_{ss} and IMP determined by LAM–ICP–MS. Figure 7 shows chemical variation as a function of position in the grain. Analyses from sample LL99–6–1 (Figs. 7a, b) show a Ms_{ss} core with low levels of Fe, V, Rb, Cs, and Ba, and high levels of Zr, Hf, Nb, and Ta relative to the IMP rim. Analyses from sample LL99–8–1 (Figs. 7c, d) and LL99–11 (Figs. 7e, f) were done on several alternating Ms_{ss}–IMP zones. Figure 8 shows covariation plots for all spots analyzed by LAM–ICP–MS (excluding one highly anomalous point). The individual Ms_{ss} and IMP compositions appear to overlap on all variation diagrams, but the averages of Ms_{ss} and IMP zones are different. Figures 8a–d show the elements positively correlated with Fe, including the transition element V and the large-ion lithophile elements Rb, Cs, and Ba, in addition to F (Fig. 6). Clearly, all these elements that are positively correlated with Fe content must also be positively correlated with each other. Figures 8e and f show that concentrations of Zr and Hf are negatively correlated with Fe. Figures 8g–i show no clear system-

atic variation of levels of Nb, Ta, or Sc with Fe. Figure 8j shows that, despite considerable variation in Zr and Hf concentration between the Ms_{ss} and IMP zones, these elements do not fractionate relative to each other, and the Zr/Hf value remains approximately constant at ~7. On the other hand, Figure 8k shows that Nb and Ta do fractionate relative to one another between Ms_{ss} (Nb/Ta ~ 10) and IMP (Nb/Ta ~ 6), albeit with considerable scatter in Ta concentrations. Furthermore, even though both Rb and Cs increase in the IMP zones, the Rb/Cs value decreases by nearly an order of magnitude from ~50 in Ms_{ss} to ~6 in IMP, meaning that these two large-ion-lithophile elements are strongly decoupled in these two micas.

Discussion

Fluorine concentrations in micas of the Lake Lewis leucogranite

The Lake Lewis leucogranite shows high concentrations of fluorine in all its mica phases (Bt_1, Bt_2, Ms_{ss}, and IMP). High-fluorine micas are common in highly evolved leucogranites (*e.g.*, Breiter 2002, Broska *et al.* 2002), and positive correlations between Fe and F contents are normal in white micas (Munoz 1984, Halter & Williams-Jones 1999). The problem of interference between Fe$L\alpha_1$ and F$K\alpha_1$ peaks is readily resolved with wavelength analysis using an LDE1 synthetic crystal

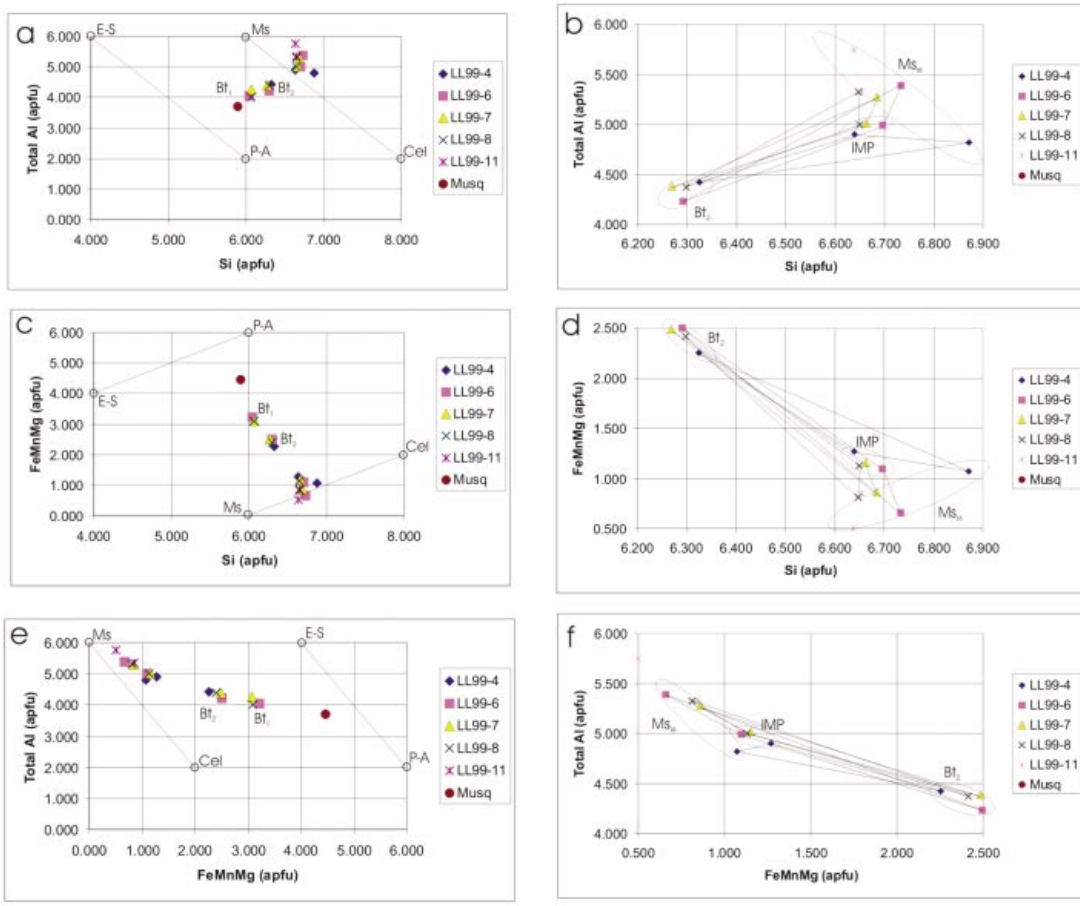

FIG. 5. Composition of Lake Lewis micas in terms of major elements. (a,c,e) Compositions of the Lewis Lake micas in relation to common mica end-members. Note the two different types of biotite: small euhedral grains included in quartz (Bt_1) lie closer to the line defining trioctahedral micas than those in the rest of the rock (Bt_2). (b,d,f) Same diagrams with expanded scales to show relations among the three main "coexisting" phases (Ms_{ss}–IMP–Bt_2). In all cases, the light brown intermediate mica phase has a composition between Ms_{ss} and Bt_2, but closer to Ms_{ss}. Symbols: Ms: muscovite, Cel: celadonite, P–A: phlogopite–annite, E–S: eastonite–siderophyllite. Sample labeled "Musq" is biotite from the relatively unfractionated Musquodoboit batholith.

and careful selection of backgrounds. As an indication of our analytical confidence, note that biotite from the much smaller and unevolved Musquodoboit batholith, located to the east of the South Mountain batholith, analyzed at the same time as the Lake Lewis micas, has amongst the highest Fe contents, but also has by far the lowest F content. Furthermore, the very high levels of fluorine in the low-Fe muscovite cannot be an interference effect because the Fe$L\alpha_1$ peak is small. The Lake Lewis leucogranite contains magmatic topaz, and it also evolved late-stage hydrothermal fluids that precipitated large quantities of fluorite. We conclude that the Lake Lewis leucogranite is a product of the crystallization of a high-F magmatic system, and that its topaz and mica compositions now reflect that chemical characteristic.

Causes of trace-element variation in Ms_{ss} and IMP

Although the major-element compositions of Ms_{ss} and IMP are distinct (Table 1, Figs. 5, 6), most trace-element variation diagrams (Fig. 8) show a continuous trend of compositions between muscovite and IMP. We interpret this continuum of trace-element compositions as an artifact of the different analytical techniques (Fig. 9). In an analysis of cleavage fragments, the electron microprobe samples to a depth of *ca.* 5 μm, whereas the penetration of LAM–ICP–MS is much deeper (*ca.* 150 μm), and light penetrates the entire crystal. In a concentrically zoned mica, we may analyze with the LAM–ICP–MS technique the two end-member zones in varying proportions; therefore, the extremes of the range

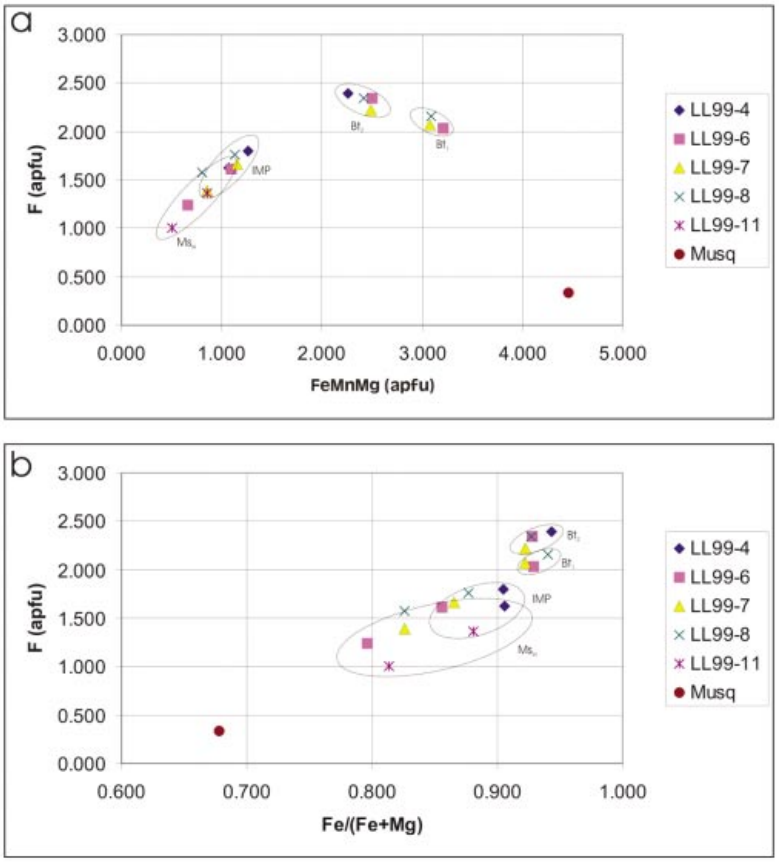

FIG. 6. Fluorine concentrations in the Lake Lewis micas. (a) As a function of Fe + Mn + Mg (*apfu*), a wide gap separates the muscovite and IMP from the biotite compositions, and the early biotite included in quartz has a distinctly lower concentration of fluorine than the main biotite of the rock. (b) As a function of Fe/(Fe + Mg), a continuum exists for all micas from the Lake Lewis leucogranite. The significantly different biotite is from the Musquodoboit batholith.

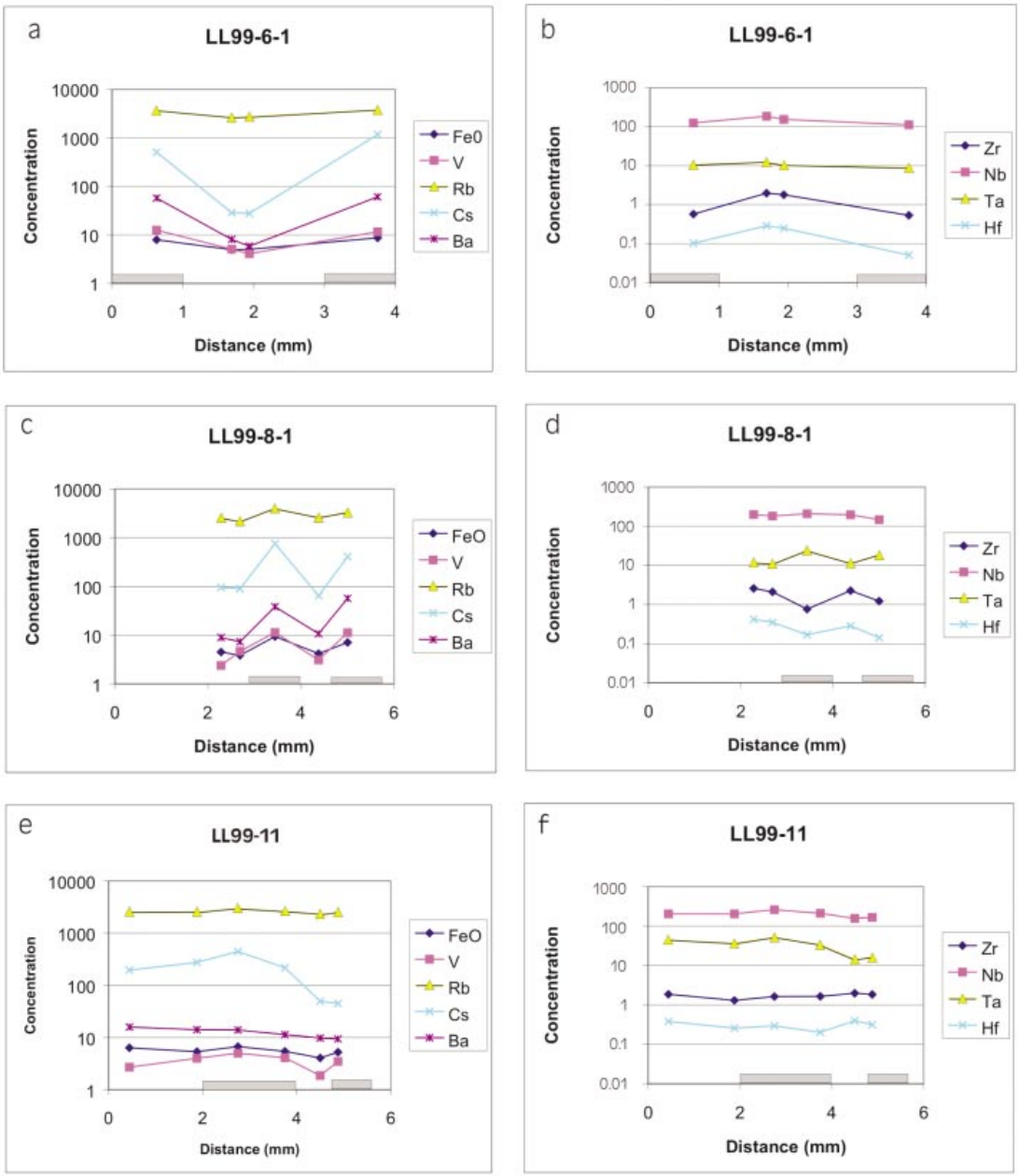

FIG. 7. Composition–distance plots for trace elements in white micas. (a, b) Sample LL99–6–1 (IMP rim – muscovite core – IMP rim). (c, d) Sample LL99–8–1 (oscillatory zones from core to rim). (e, f) Sample LL99–11 (oscillatory zones from core to rim). Concentrations are in oxide weight percent for FeO, and parts per million for the other elements. Shaded bars on the horizontal axes represent the IMP zones.

TABLE 2. TRACE-ELEMENT CONCENTRATIONS IN Ms_{ss} AND IMP MICAS, LAKE LEWIS LEUCOGRANITE PLUTON, NOVA SCOTIA

Sample	Color	FeO	Sc	V	Ga	Rb	Sr	Zr	Hf	Nb	Ta	Ba	Cs
Batch 1													
LL99-6ICPMS1a	d	6.76	24.9	11.0	133	2982	0.2	1.5	0.3	181	17.5	12.2	178
LL99-6ICPMS1b	d	7.58	24.8	11.5	87	3118	0.3	0.6	0.1	103	9.1	62.3	710
LL99-6ICPMS1c	l	5.57	15.9	5.2	128	2395	0.1	1.7	0.2	144	11.9	8.2	60
LL99-6ICPMS1d	l	5.51	14.8	3.2	121	2437	0.2	1.5	0.3	135	11.2	6.1	40
LL99-6ICPMS2a	d	8.43	28.7	16.4	105	2950	0.3	1.0	0.1	128	13.9	42.6	577
LL99-6ICPMS2b	l	6.01	16.4	7.6	123	2645	0.2	1.4	0.3	145	12.3	14.4	139
LL99-6ICPMS2c	l	4.41	14.1	5.9	122	2255	0.1	1.9	0.3	148	11.9	7.4	36
LL99-8ICPMS1a	l	3.70	33.2	1.3	155	2061	0.2	2.0	0.4	177	10.4	4.9	22
LL99-8ICPMS1b	d	4.16	32.0	1.8	143	2134	0.1	2.0	0.3	178	10.9	8.2	39
LL99-8ICPMS1c	l	4.52	17.2	2.4	141	2614	0.1	2.1	0.3	190	12.3	4.2	40
LL99-8ICPMS1d	d	6.35	30.6	5.2	155	3156	0.2	1.6	0.3	214	26.8	7.7	109
LL99-8ICPMS2a	d	4.67	19.4	3.5	151	2416	<0.1	2.0	0.3	151	10.6	8.0	26
LL99-8ICPMS2b	l	4.84	17.9	2.7	123	2346	0.1	2.1	0.4	140	9.6	6.2	31
LL99-8ICPMS2c	d	5.13	17.3	4.9	133	2517	0.2	1.7	0.2	148	11.2	7.8	39
LL99-11ICPMS1a	*	----	10.1	0.7	106	1638	0.3	1.2	0.2	95	10.1	9.1	36
LL99-11ICPMS1b	d	6.68	19.7	4.4	93	2235	0.6	1.2	0.2	168	25.8	11.0	308
LL99-11ICPMS1c	l	1.09	<8.3	1.4	19	399	10.3	31.7	0.8	27	4.0	65.9	33
LL99-11ICPMS1d	d	4.06	15.5	1.5	92	1711	0.3	1.3	0.2	104	10.2	9.2	59
LL99-11ICPMS1e	d	6.39	21.3	2.0	118	2813	0.8	1.3	0.3	143	27.5	12.6	407
Batch 2													
LL99-6ICPMS1a	d	7.93	15.4	12.5	87	3608	0.3	0.6	0.1	125	10.6	57.5	509
LL99-6ICPMS1b	l	4.95	12.3	5.1	119	2588	0.3	2.0	0.3	186	12.4	8.1	29
LL99-6ICPMS1c	l	5.04	13.0	4.1	118	2712	<0.2	1.8	0.2	154	10.2	5.8	28
LL99-6ICPMS1d	d	8.70	14.8	11.6	85	3726	0.4	0.5	0.1	113	8.8	60.7	1175
LL99-6ICPMS2a	d	9.23	18.5	13.1	94	3427	0.4	0.6	0.1	152	14.0	44.3	507
LL99-6ICPMS2b	l	6.90	23.3	14.3	126	3069	<0.3	1.6	0.2	206	16.1	12.2	78
LL99-6ICPMS2c	d	5.50	19.4	9.5	115	2662	0.3	1.9	0.3	226	23.2	12.4	73
LL99-8ICPMS1a	l	4.47	27.6	2.4	125	2524	0.3	2.6	0.4	197	11.6	8.9	94
LL99-8ICPMS1b	l	3.84	30.8	4.7	109	2115	<0.2	2.1	0.3	181	10.7	7.3	89
LL99-8ICPMS1c	d	9.35	18.2	11.3	117	3927	0.2	0.8	0.2	208	23.3	38.2	749
LL99-8ICPMS1d	l	4.16	14.6	3.1	127	2573	0.4	2.3	0.3	196	11.2	10.7	64
LL99-8ICPMS1e	d	7.04	13.6	11.2	83	3268	0.3	1.2	0.1	146	18.0	57.0	407
LL99-8ICPMS2a	d	4.88	12.9	3.8	140	2882	<0.2	2.1	0.3	192	11.3	8.3	30
LL99-8ICPMS2b	l	4.71	12.6	3.4	125	2812	<0.2	2.0	0.3	185	11.3	7.4	30
LL99-8ICPMS2c	d	4.96	15.0	4.1	121	2916	<0.1	2.1	0.3	199	12.9	8.5	45
LL99-11ICPMS1a	l	6.32	<12.9	2.7	76	2490	0.8	1.9	0.4	205	44.0	15.9	194
LL99-11ICPMS1b	d	5.36	10.3	4.0	102	2479	0.6	1.3	0.3	203	36.1	14.1	275
LL99-11ICPMS1c	d	6.69	14.0	5.0	108	2938	0.5	1.6	0.3	260	50.8	13.9	445
LL99-11ICPMS1d	d	5.45	19.6	4.1	106	2586	<0.4	1.6	0.2	211	32.9	11.4	216
LL99-11ICPMS1e	l	4.06	20.6	1.9	123	2266	<0.4	2.0	0.4	157	14.1	9.7	49
LL99-11ICPMS1f	l	5.21	22.5	3.5	123	2443	<0.3	1.9	0.3	166	15.7	9.4	45

Symbols: d: dark, l: light, * indeterminate as to color; the label refers to the relative appearance of cleavage fragments in transmitted plane-polarized light, and correlates approximately to Ms_{ss} and IMP, respectively (Fig. 9). The trace-element data were acquired in two batches by the LAM–ICP–MS technique, and are expressed in ppm. ----: no data available.

of compositions probably best represent the compositions of Ms_{ss} and IMP. Furthermore, we have no trace-element data for the biotite, but for all other elements, IMP is intermediate between Ms_{ss} and Bt_2. With these caveats in mind, we examine the broad trace-element variations.

The positive Fe–V correlation from Ms_{ss} to IMP parallels that in the whole rocks and is consistent with the trend produced by fractional crystallization from a differentiating magma, but the positive Fe–Ba, –Rb, and –Cs correlations seem to be anomalous. Similarly, the negative Fe–Zr, –Hf correlations are at variance with those expected from fractional crystallization. Although the Zr/Hf value remains constant in the two micas, the Nb/Ta and Rb/Cs values are significantly different. If we cannot explain the trace-element differences between the closely associated Ms_{ss} and IMP by fractional crystallization, perhaps the answer lies either in the mica structure or the prevailing conditions in the magma.

In terms of major-element compositions and octahedral site occupancies, Ms_{ss} and IMP are very similar. We do not believe that the structures are so different as to accommodate higher concentrations in IMP of elements as geochemically different as V and Ba, or Ta and Cs. Instead, the compositions may reflect different conditions in the magma. The high Rb and F, low Zr, Hf, and Na/(Na + K), and significant changes in Nb/Ta and Rb/Cs of the IMP, may be consistent with appearance of a fluid phase, for which the silicate melt/fluid phase partition coefficients are not unity. For example, the high-field-strength elements (Zr, Hf) are probably only weakly partitioned into the fluid phase; therefore, the appearance of a fluid has little effect on Zr/Hf in the melt and the micas that crystallize from it (*cf.* Bau 1996). However, for the large-ion-lithophile elements that are variably partitioned into the fluid, the melt and micas that crystallize from it may show considerable difference in large-ion-lithophile element ratios. Although Nb/Ta is ~4 in granites, granite-related hydrothermal mineral deposits show considerable variation in Nb/Ta values, indicating that these elements do fractionate relative to one another in the presence of a fluid phase. An IMP that crystallizes from a fluid-saturated melt, therefore, may be enriched or depleted in certain elements, depending on how strongly they have been partitioned into the fluid. We suggest that the principal reason for the trace-element differences between the Ms_{ss} and IMP zones is variable partitioning in the Ms_{ss}–IMP–melt and Ms_{ss}–IMP–melt–fluid systems. If this interpretation of the Ms_{ss}–IMP zoning is correct, the IMP zones should contain primary fluid inclusions, whereas the Ms_{ss} zones should not. A cursory examination of few zoned grains shows fluid inclusions in both types of zone but, at this stage of the investigation, we do not know if these inclusions are primary or secondary in origin.

Origin of micas in the Lake Lewis leucogranite

The small, subhedral to euhedral grains of biotite, Bt_1, isolated in quartz, also have the most normal-looking high-Fe (~21 wt.% FeO) chemical compositions. To advocate that the Bt_1 grains are anything but early magmatic in origin would be difficult.

The origin of the larger anhedral to euhedral grains of biotite, Bt_2, constituting part of the matrix of the leucogranites, is more problematic. The grain-size compatibility of Bt_2 with other magmatic minerals (*e.g.*, quartz and feldspars) in these leucogranites, the subhedral to euhedral shapes of the grains, and the straight, optically sharp grain-boundaries, especially against IMP, suggest that Bt_2 also is magmatic in origin. The reason for the substantially lower iron (~16 wt.% FeO) and slightly higher fluorine in Bt_2 relative to Bt_1 is not immediately apparent (but see below).

In general terms, the Ms_{ss} of the Lake Lewis leucogranite is also generally compatible in size with acknowledged magmatic minerals in the leucogranite [although we have preferentially selected larger grains (Fig. 3) for LAM–ICP–MS work]. Many euhedral to subhedral grains of white mica are also compatible in shape with crystallization from a silicate melt. Euhedral to subhedral inclusions of white micas are also present in magmatic plagioclase, K-feldspar, and quartz, suggesting a similar primary magmatic origin for the white micas. Ortoleva (1994) showed that euhedral habits alone do not demand unobstructed crystallization from a melt, but the sizes and shapes of the micas are consistent with crystallization of the other (magmatic) minerals, namely quartz and the feldspars.

Using a chemical approach, Ham & Kontak (1988) established good correlations between the trace-element concentrations in the muscovite and the whole-rock compositions, and concluded that the muscovite could not be secondary. A further test of the primary nature of the muscovite is to use its trace element contents with known muscovite–melt partition coefficients (Icenhower & London 1995, Raimbault & Burnol 1998) to calculate the composition of the coexisting melt. This comparison is fraught with analytical problems, assumptions about whole rocks approximating the compositions of melts, and the suitability using the average Lake Lewis leucogranite composition (Clarke *et al.* 1993) as the comparator. We conclude, on strong textural and weaker chemical grounds, that the Ms_{ss} crystals of the Lake Lewis leucogranite are primary magmatic.

Figures 2–4 show that IMP occurs mainly as epitactic overgrowths on Bt_2 and Ms_{ss} (it also occurs as an apparent reaction-induced rim on primary magmatic topaz). The Ms_{ss}–IMP grain boundaries (Figs. 3, 4) are more consistent with primary magmatic overgrowths or reaction relationships than, say, low-temperature hydro-

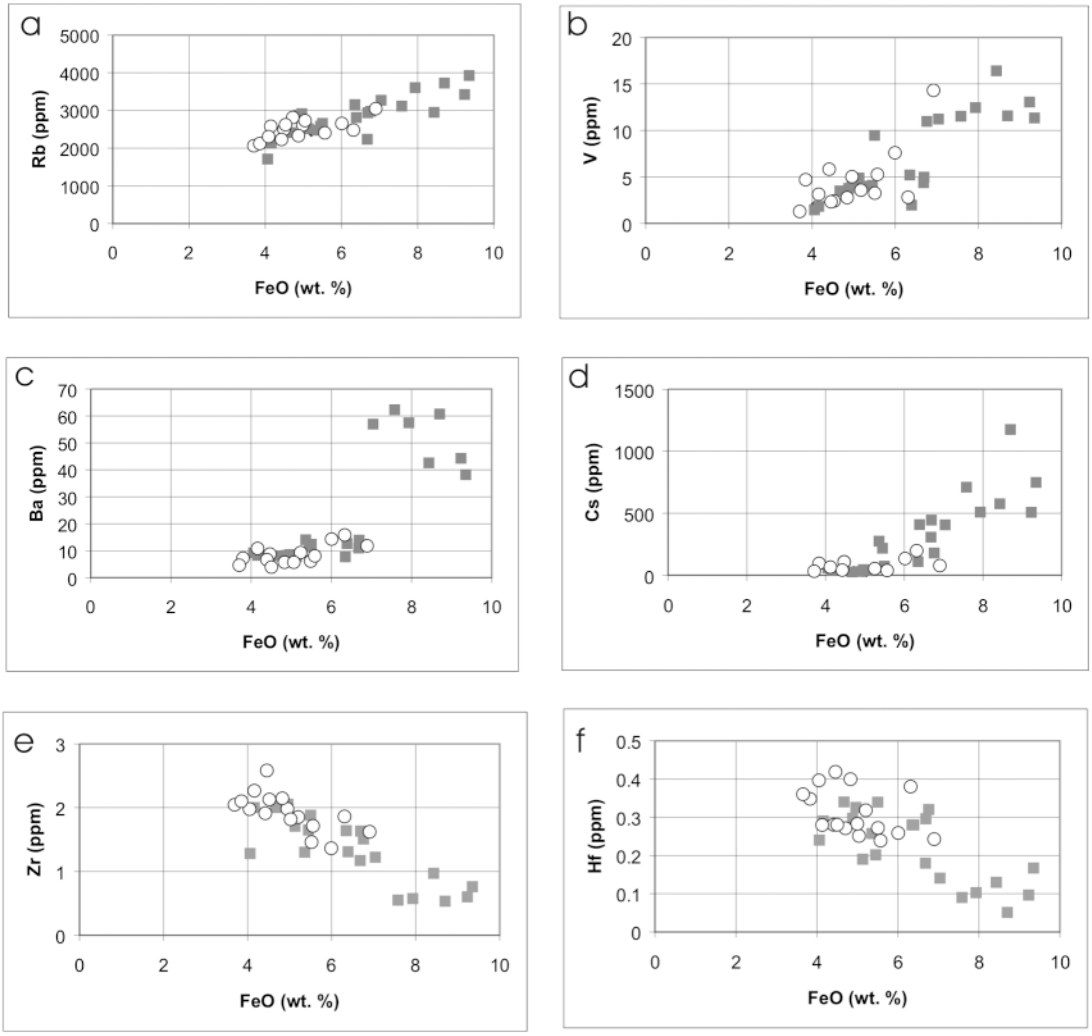

thermal alteration. Also, secondary hydrothermal alteration cannot explain how selective replacement of internal bands of muscovite in a single crystal could occur.

The IMP is intermediate in composition between the Bt_2 and Ms_{ss} it overgrows, but is much closer to the composition of the muscovite than of the biotite (Figs. 5, 6). If the bulk composition of IMP reflects approximately the modally weighted average composition of Ms_{ss} and Bt_2 before the IMP began growing, the bulk chemical composition of the mica is approximately the same under both sets of conditions. The appearance of the single IMP phase, instead of Bt_2 and Ms_{ss}, may indicate that the solvus between Bt_2 and Ms_{ss} did not exist. If the Bt_2 and Ms_{ss} are magmatic, and if the system alternates between these normal micas and IMP, the conclusion seems inescapable that IMP also is magmatic, or fluid–magmatic, in origin.

The variably mottled appearance of the IMP in BSE images suggests that this mineral is heterogeneous with respect to the distribution of iron (Figs. 2, 4). Detailed electron-microprobe analyses show IMP to consist of mica compositions varying from Ms_{ss} to Bt_2. Either this heterogeneity is an original growth-induced feature, or a formerly homogeneous IMP has broken down or undergone exsolution. Ferrow *et al.* (1990) described exsolution in Fe-rich white mica from the Lawler Peak granite in Arizona, and Ferraris *et al.* (2001) have described exsolution lamellae of phlogopite–eastonite in muscovite. If exsolution has occurred in the Lake Lewis IMP phase, the extent of this exsolution is variable from

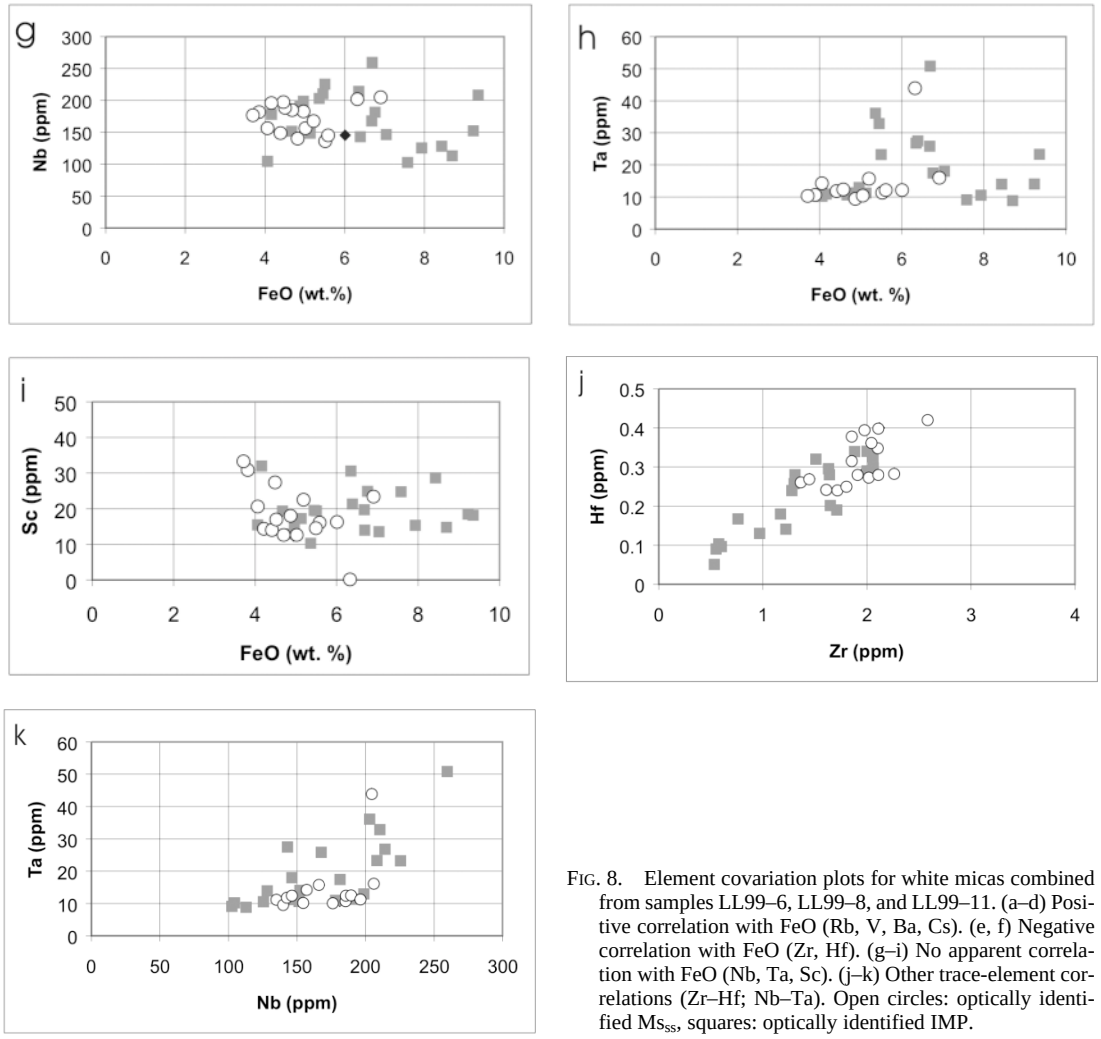

FIG. 8. Element covariation plots for white micas combined from samples LL99–6, LL99–8, and LL99–11. (a–d) Positive correlation with FeO (Rb, V, Ba, Cs). (e, f) Negative correlation with FeO (Zr, Hf). (g–i) No apparent correlation with FeO (Nb, Ta, Sc). (j–k) Other trace-element correlations (Zr–Hf; Nb–Ta). Open circles: optically identified Ms_{ss}, squares: optically identified IMP.

sample to sample. Alternatively, if the mottled appearance were the result of some kind of alteration, we cannot explain why the Ms_{ss} and Bt_2 in the same rock have remained homogeneous and unaffected.

In summary, Hogan (1996, p. 156) noted that minerals "can alternate as reactants or products in different reactions, accounting for textures indicating multiple periods of crystallization separated by resorption". Many rocks in the Lake Lewis leucogranite contain four texturally and chemically distinct primary magmatic micas (*e.g.*, samples LL99–6,7,8). These micas cannot, however, represent an equilibrium assemblage and must, therefore, represent different times and conditions of crystallization of the leucogranitic magma. Bt_1 is an early, perhaps pre-muscovite, magmatic phase with its composition unconstrained by that of any other coexisting mica. Similarly, three stable coexisting micas in a single rock are also unlikely. We regard Bt_2 + Ms_{ss} as the normal coexisting mica pair, leaving IMP as the anomalous phase. Petrographic observations in LL99–7, for example, show clear Bt_2–IMP–Bt_2 and Ms_{ss}–IMP–Ms_{ss} mantling relationships. Although it is not possible to uniquely determine the relations, either Bt_2 and Ms_{ss} together, or IMP alone, seem to have been stable. These epitactic mantling textures suggest a type of "mica rapakivi" relationship (although no such true rapakivi relation exists among the coexisting plagioclase and alkali feldspar in these rocks). The IMP seems to have grown in favor of both biotite and muscovite during alternating stages in the crystallization history of the

pluton. When ambient conditions returned, the crystallization of biotite and muscovite resumed, and the IMP became unstable and broke down.

Causes of oscillatory epitactic zoning

The epitactic zoning of micas (Bt_2 ↔ IMP and Ms_{ss} ↔ IMP) in the Lake Lewis leucogranite suggests that: (i) The mica crystals were responding to changing T–P–*X* (temperature – pressure – composition) conditions in the system. (ii) The straight, optically sharp, boundaries between epitactic zones suggest that the controlling T–P–*X* conditions changed more rapidly than chemical reactions involving exchange equilibria. (iii) The irregular, optically diffuse boundaries between epitactic zones suggest that the controlling T–P–*X* conditions changed slowly enough to allow some chemical exchange to take place. (iv) The T–P–*X* conditions were fluctuating repeatedly to produce the oscillations. (v) The entire system ultimately failed to reach chemical equilibrium.

In detail, driving forces of these epitactic overgrowths in the Lake Lewis leucogranite include changes in T, P or *X*, as follows.

Changes in T. Figures 2 and 4 show that, in part at least, the epitactically zoned micas grew in regions of a magma at an advanced stage of crystallization; therefore, at least some zones formed under conditions of static spatial coordinates in the magma chamber. If the epitactically zoned micas of the Lake Lewis leucogranite are the result of temperature fluctuations, then the oscillating ΔT must be taking place *in situ*. Presumably, this low-probability event could happen only with repeated influxes of new magma nearby, and the zoned micas would have formed in response to thermal oscillations.

Changes in P. As with temperature above, if the epitactically zoned micas of the Lake Lewis leucogranite are the result of pressure fluctuations, then the oscillating ΔP must be taking place *in situ.* Only an increase in fluid pressure, when the magma evolves a separate volatile phase, could bring about such a change. Theoretically at least, such fluid-generated overpressures could be tens of kilobars (Burnham 1979), but in practice the limiting condition may be the tensile strength of the surrounding rocks, which may only be in the order of 0.05–0.25 kilobars (Blake 1984, Schmitt 2001).

Velde (1965, 1980) and Green (1981) discussed the conditions of a fluid-bearing magma, and clearly demonstrated an increase in phengitic substitution in white micas with increasing H_2O pressure. The Lake Lewis IMP is not more phengitic than the Ms_{ss} it overgrows but, like high-pressure phengite, it does have significantly lower Na/(Na + K) than the muscovite in these rocks. [For the three samples containing four micas, Na/(Na + K) = 0.036, 0.040, 0.092, and 0.055 for Bt_1, Bt_2, Ms, and IMP, respectively]. The phengite geobarometer (Massonne & Schreyer 1989, Massonne & Szpurka 1997, Domanik & Holloway 2000), even if it were applicable to the Ms_{ss}–IMP pair, is not calibrated for the leucogranite system. Thus, even if fluid overpressures are responsible for these IMP epitactic zones, we currently cannot know either the absolute pressure associated with the IMP zones, or even the ΔP associated with the Ms_{ss}–IMP reversals.

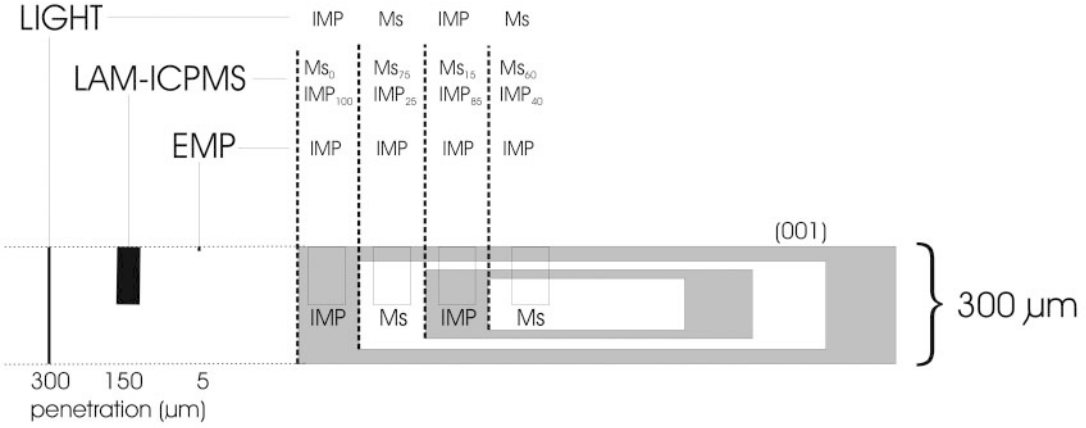

FIG. 9. Schematic diagram of a chemically zoned cleavage fragment of white mica, cut perpendicular to (001), to explain the lack of correlation between optical, EMP, and LAM–ICP–MS observations. Light penetrates the entire thickness of the grain and, in plane-polarized light, the mica will approach colorless for muscovite (Ms, white), and be various hues of light brown for the intermediate mica phase (IMP, shaded). The laser-ablation microprobe does not necessarily sample the same two phases in the same proportions. The electron microprobe has limited penetration and, in this example, "sees" only IMP. As a consequence, optical, LAM–ICP–MS, and EMP observations may not always agree.

Changes in X. A variety of changes in the chemical environment might be responsible for the development of the oscillatory zoning in biotite and muscovite in the Lake Lewis leucogranite, including *changes in magma composition*. Roycroft (1989) considered that subtle changes in magma composition were responsible for the oscillatory zoning of white micas in the Leinster granite. That the epitactic overgrowths could be the products of H_2O-undersaturated magmatic processes is problematic, because there is no apparent reason why the bulk composition of the magma would fluctuate enough to alternate between Ms_{ss}–Bt_2 crystallization and IMP crystallization. Also, because some of the zoning in the micas of the Lake Lewis leucogranite apparently formed *in situ*, we consider any influx of new magma under such conditions of advanced crystallization as unlikely.

Monier & Robert (1986b) noted that the miscibility gap between coexisting dioctahedral and trioctahedral micas shrinks with increasing lithium (and fluorine) concentrations. All Lake Lewis micas have high measured F contents, and the IMP phase in particular has high calculated Li contents. We cannot determine if high Li is the cause of the single IMP phase, or if the single IMP phase is a consequence of some other control.

It is possible that there was *double diffusion of heat and material*. The phenomenon of double diffusion of heat and material to produce Liesegang bands is well known in experimental chemistry, and has been applied to geological situations (*e.g.,* Cabarcos *et al.* 1996, Ortoleva 1994). Crystallizing Bt_2 could create a zone of iron-depleted melt around it, resulting in the nucleation of IMP, and crystallizing Ms_{ss} could create a zone of iron-enriched melt around it, also resulting in the nucleation of IMP, but the widths of the zones in the Lake Lewis micas are greater than those normally associated with Liesegang bands. Furthermore, if such a double-diffusion mechanism were responsible, such epitactic textures should be common in all two-mica granites.

Gomes & Neiva (2000) interpreted the simple cores of muscovite with a phengitic rim in a pegmatite in the Ervedosa granite, Portugal, as the result of a period of *hydrothermal alteration*. The primary magmatic origin of the Lake Lewis micas suggests, however, that the entire process of oscillatory epitactic growth has to be accomplished above the leucogranite's solidus.

It also is possible that variations in *oxygen fugacity* played a role. Without knowledge of the Fe^{3+} contents of these micas, however, we are unable to assess the possible effects of $\Delta f(O_2)$.

Finally, significant variations in *activity of H_2O* can be expected; conditions may well have alternated between $a(H_2O) < 1$ (H_2O-undersaturated, fluid-absent magma, P = lithostatic) to $a(H_2O) = 1$ (H_2O-saturated, fluid-present magma, P > lithostatic). Such a chemical, and pressure, variation could easily be transmitted to all minerals crystallizing in the pluton.

In conclusion, we believe that increasing fluid pressure, with or without differential trace-element partitioning into a fluid phase, may provide the pluton-wide physical and chemical changes needed to produce the epitactically zoned micas. Alternating lithostatic and fluid-overpressured conditions may be responsible for the oscillatory trace-element zoning in the Lake Lewis leucogranite micas. We are inclined to believe that the normal lithostatic condition produced $Bt_2 + Ms_{ss}$, and that the IMP is associated with the anomalous fluid-overpressured condition. But did IMP grow as the pressure increased, at the high-pressure conditions, or by pressure quenching during a catastrophic return to lithostatic (or even hydrostatic) pressure conditions? Potentially, the $Ms_{ss} \rightarrow$ IMP, IMP $\rightarrow Ms_{ss}$, $Bt_2 \rightarrow$ IMP, and IMP $\rightarrow Bt_2$ grain boundaries could help to answer this question. Ideally, straight, optically sharp boundaries between epitactic zones should represent rapid changes in conditions, whereas irregular, optically diffuse boundaries between epitactic zones should represent gradual changes in conditions, but there appears to be nothing systematic about the diffuse or sharp nature of these contacts (*i.e.*, any of the four possible contacts can be sharp or diffuse).

Implications of the epitactically zoned micas

If the Ms_{ss} and Bt_2 zones represent low $P(H_2O)$, and the IMP zones represent high $P(H_2O)$ magma, then the epitactically zoned $Ms_{ss} \leftrightarrow$ IMP and $Bt_2 \leftrightarrow$ IMP micas may serve as uncalibrated, recording-type H_2O-pressure gauges on the hydraulic pump that may have produced secondary alteration and mineral deposits elsewhere. If these epitactically zoned micas represent alternating build-up and release of H_2O pressure, then the release of that H_2O can have physical and chemical implications in the surrounding rocks (Fournier 1999). Physically, at high fluid overpressures, the surrounding rocks may expand and fracture, causing the observed cataclasis in some of the Lake Lewis leucogranitic rocks, similar to the explosive magmatic breccias in the Podlesí stock in the Czech Republic (Breiter 2002). Fossil escape routes for the fluid phase in granites generally may consist of fractures, veins, zoned aplite–pegmatites, and comb-textured pegmatites (Lowenstern & Sinclair 1996). Chemically, the fluid appears to have carried high concentrations of Ca, Fe, Li, and F to produce siderophyllite–protolithionite alteration of muscovite and fluorite-coated fractures in host rocks (Bogutyn 2001), as well as metals such as Mo to produce the minor molybdenite-bearing pegmatites in the Lake Lewis leucogranite and possibly the larger Walker Moly aplite – pegmatite – greisen nearby (Fig. 1). Webster (1990) argued that F-rich fluids could transport granophile elements (Sn, W, U, Mo) typical of those occurring in mineral deposits in the SMB. The East Kemptville topaz–cassiterite greisen at the southwestern end of the

SMB is a clear example of the ability of F-rich fluids to move granophile elements (Richardson *et al.* 1990, Halter *et al.* 1998a, b). Furthermore, the clear separation of the two geochemically similar elements, Nb and Ta, between the muscovite and IMP zones has implications for the wide Nb/Ta compositional variation in granite-related Nb–Ta mineral deposits (Horng *et al.* 1999, Pelrine 2003).

Finally, although the muscovite–phengite geobarometer is generally inappropriate for granitic rocks, the compositional differences between epitactic zones is significant (suggesting a large ΔP), and many epitactic zone boundaries are sharp (suggesting rapid changes in pressure conditions). In the extreme, overpressure release may have taken place by large eruptions of ignimbrite above the South Mountain Batholith. Such intensive fracturing of the batholithic roof would have provided upward pathways for the ascent of felsic magma (rhyolite dykes, or "elvans") and downward pathways for the incursion of meteoric water into the late-stage mineral deposits of the SMB (Carruzzo *et al.* 2000).

In summary, the model of alternating build-up and release of H_2O pressure in the late stages of crystallization of the SMB (Fig. 10), as exemplified by the Lake Lewis leucogranite, can explain:

- epitactically zoned micas, by a combination of pressure build-up and changing melt–fluid partition coefficients
- cataclastic rocks in the Lake Lewis leucogranite and in adjacent rocks (*e.g.*, the "jasper breccia" near New Ross), apparently broken by explosive release of pressure
- fractured endocontact rocks with fluorite coatings as a product of explosive release of pressure involving a fluorine-rich fluid
- kinked muscovite, expanded and injected with fluorite along cleavage planes, and altered to siderophyllite–protolithionite with fluorite in the pluton and surrounding rocks
- internal stockwork of veins and pegmatites in the pluton as fossil fluid-escape pathways
- rhyolite dykes ("elvans"), such as in the Massif Central (Raimbault & Burnol 1998), in the Turner tin deposit as evidence of rapid ascent of felsic magma to the surface (however, countered by the apparent absence of rhyolite pebbles in the Horton conglomerate overlying the SMB)
- aplite – pegmatite – greisen mineralization in surrounding plutons (Walker Moly deposit)
- late-stage influx of meteoric water into the South Mountain Batholith.

Conclusions

The Lake Lewis leucogranites have whole-rock chemical compositions that lie at the most evolved end of the well-defined magmatic fractionation trend of the South Mountain Batholith. Textural and chemical evidence suggests that all four of its micas have a magmatic origin, or an origin involving a fluid-bearing magma. Bt_1 is an early, relict, pre-muscovite, primary magmatic phase. Bt_2, the second magmatic biotite, grew in equilibrium with primary magmatic Ms_{ss}. The Ms_{ss} + Bt_2 pair, and epitactic IMP overgrowths, are all magmatic minerals that resulted from alternating low and high fluid pressures in the magma. Such micas with oscillatory zoning thus serve as uncalibrated recording-type pressure gauges. Proximally, the epitactically zoned micas correlate locally with hydrothermal alteration, aplite – pegmatite – greisen mineralization, and cataclasis. Distally, the epitactically zoned micas may correlate with rhyolite dykes ("elvans"), putative eruptive ignimbrite sheets, and influxes of meteoric water into the pluton. If zoned micas can be equated with high-pressure hydrothermal fluids, then their presence may be a prospecting tool for granophile-element-enriched mineral deposits.

Acknowledgements

We gratefully acknowledge the assistance of Robert MacKay in the electron microprobe laboratory at Dalhousie University, and Jianzhong Fan in the LAM–ICP–MS laboratory at the University of Victoria. Barrie Clarke acknowledges the essential support through a Research Grant from the Natural Sciences and Engineering Research Council of Canada. Sarah Carruzzo and Linda Ham generously offered helpful comments on a preliminary version of the manuscript, and Saskia Erdmann, Penny King, Dave Pattison, Trond Slagstad, and E-an Zen offered constructive comments during formal and informal discussions. For their detailed and constructive reviews, we are grateful to Hans-Jürgen Förster and Robert F. Martin.

FIG. 10. Hypothetical model for the formation of epitactically zoned biotite and muscovite in the Lake Lewis leucogranite. The three stages of magmatic evolution, from left to right, are recognized. (a) Normal conditions: H_2O-undersaturated magma, lithostatic pressure. Bt_2 and Ms_{ss} crystallize with compositions on the limbs of a solvus curve. (b) Overpressured conditions, H_2O-saturated

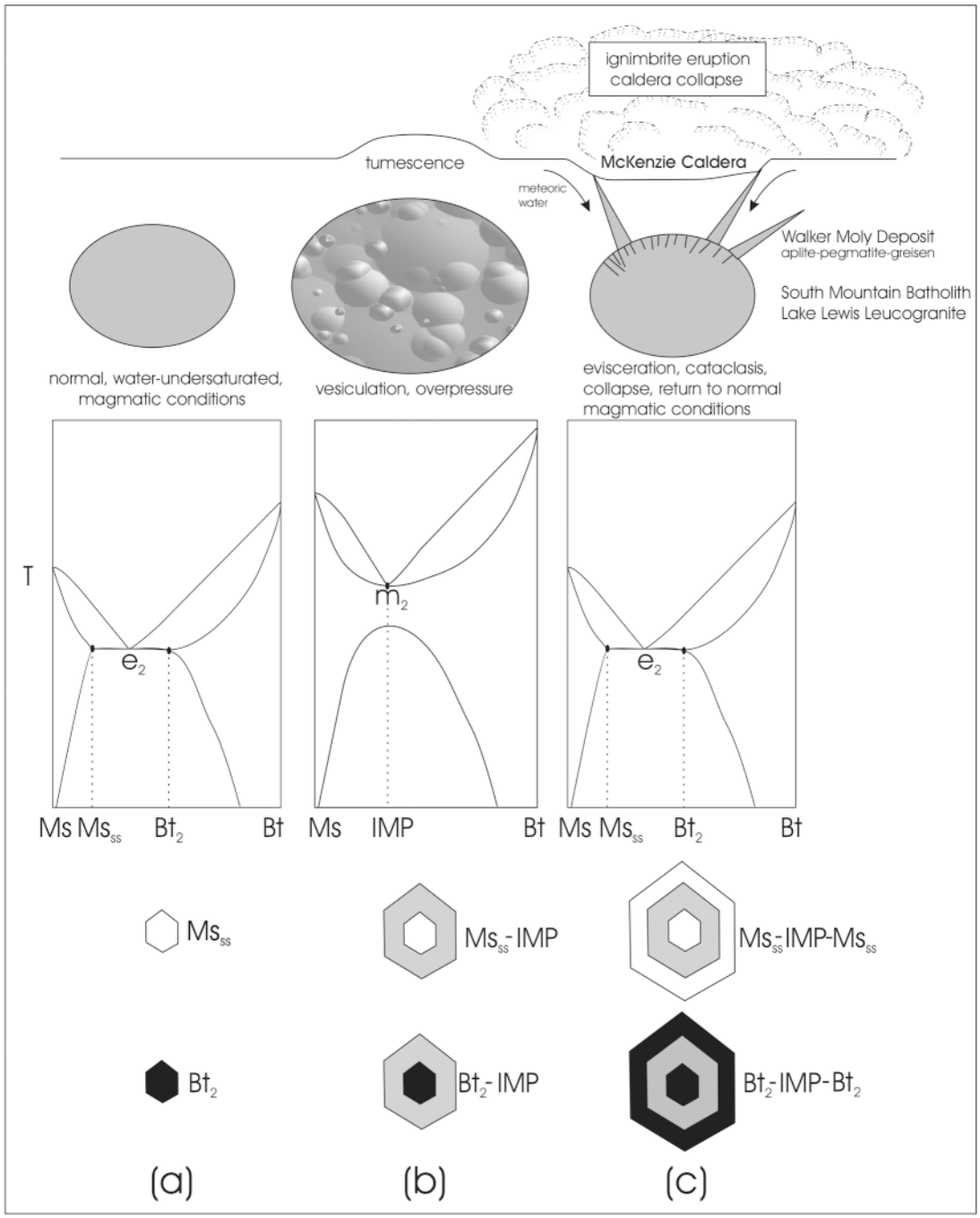

magma: solidus and solvus curves do not intersect on the schematic pseudobinary phase diagram for mica. IMP crystallizes because of increasing pressure, high pressure, or catastrophically decreasing pressure. (c) Normal conditions, fluid overpressure released by failure of roof rocks, return to crystallization of Bt_2 and Ms_{ss}, cataclasis of local rocks, possible ignimbrite eruption, emplacement of rhyolite dykes (elvans), formation of hydrothermal mineral deposits, hydrothermal alteration, influx of meteoric water into magma chamber. The name of the hypothetical "McKenzie Caldera" recognizes the advent of modern petrological studies on the South Mountain Batholith (McKenzie 1974).

References

BAU, M. (1996): Controls on the fractionation of isovalent trace elements in magmatic and aqueous systems; evidence from Y/Ho, Zr/Hf, and lanthanide tetrad effect. *Contrib. Mineral. Petrol.* **123**, 323-333.

BLAKE, S. (1984): Volatile oversaturation during the evolution of silicic magma chambers as an eruption trigger. *J. Geophys. Res.* **89**, 8237-8244.

BOGUTYN, P.A. (2001): *White Micas in the Lake Lewis Leucogranite, Nova Scotia*. B.Sc. Honours thesis, Dalhousie Univ., Halifax, Nova Scotia.

BREITER, K. (2002): From explosive breccia to unidirectional solidification textures: magmatic evolution of a phosphorus- and fluorine-rich granite system (Podlesí, Krušné hory Mts., Czech Republic). *Bull. Czech Geol. Surv.* **77**, 67-92.

BROSKA, I., KUBIŚ, M., WILLIAMS, C. T. & KONEČNÝ, P. (2002): The compositions of rock-forming and accessory minerals from the Gemeric granites (Hnilec area, Gemeric Superunit, western Carpathians). *Bull. Czech Geol. Surv.* **77**, 147-155.

BURNHAM, C.W. (1979): The importance of volatile constituents. *In* The Evolution of the Igneous Rocks: Fiftieth Anniversary Perspectives (H.S. Yoder Jr., ed.). Princeton University Press, Princeton, N.J. (439-482).

CABARCOS, E.L., KUO, CHEIN-SHIU, SCALA, A.. & BANSIL, R. (1996): Crossover between spatially confined precipitation and periodic pattern formation in reaction diffusion systems. *Phys. Rev. Lett.* **77**, 2834-2837.

CARRUZZO, S., KONTAK, D.J. & CLARKE, D.B. (2000): Granite-hosted mineral deposits of the New Ross area, South Mountain Batholith, Nova Scotia, Canada: P, T, and X constraints of fluids using fluid inclusion thermometry and decrepitate analysis. *Trans. R. Soc. Edinburgh: Earth Sci.* **91**, 303-319.

CHATTERJEE, N.D. & JOHANNES, W. (1974): Thermal stability and standard thermodynamic properties of synthetic $2M_1$-muscovite, $KAl_2[AlSi_3O_{10}(OH)_2]$. *Contrib. Mineral. Petrol.* **48**, 89-114.

CLARKE, D.B., MACDONALD, M.A., REYNOLDS, P.H. & LONGSTAFFE, F.J. (1993): Leucogranites from the eastern part of the South Mountain Batholith, Nova Scotia. *J. Petrol.* **34**, 653-679.

_____ & MUECKE, G.K. (1985): Review of the petrochemistry and origin of the South Mountain Batholith and associated plutons, Nova Scotia, Canada. *In* High Heat Production (HHP) Granites, Hydrothermal Circulation and Ore Genesis (C. Halls, ed.). Institute of Mineralogy and Metallurgy, London, U.K. (41-54).

DING, Y. (1995): *AFM Minerals in the Halifax Pluton.* M.Sc. thesis, Dalhousie Univ., Halifax, N.S.

DOMANIK, K.J. & HOLLOWAY, J.R. (2000): Experimental synthesis and phase relations of phengitic muscovite from 6.5 to 11 GPa in a calcareous metapelite from the Dabie mountains, China. *Lithos* **52**, 51-77.

FERRARIS, C., GROBETY, B. & WESSICKEN, R. (2001): Phlogopite exsolutions within muscovite: a first evidence for a higher temperature re-equilibration, studied by HRTEM and AEM techniques. *Eur. J. Mineral.* **13**, 15-26.

FERROW, E.A., LONDON, D., GOODMAN, K.S. & VEBLEN, D.R. (1990): Sheet silicates of the Lawler Peak granite, Arizona: chemistry, structural variations, and exsolution. *Contrib. Mineral. Petrol.* **105**, 491-501.

FOURNIER, R.O. (1999): Hydrothermal processes related to movement of fluid from plastic into brittle rock in the magmatic-epithermal environment. *Econ. Geol.* **94**, 1193-1211.

GOMES, M.E.P. & NEIVA, A.M.R. (2000): Chemical zoning of muscovite from the Ervedosa granite, northern Portugal. *Mineral. Mag.* **64**, 347-358.

GREEN, T.H. (1981): Synthetic high-pressure micas compositionally intermediate between the dioctahedral and trioctahedral mica series. *Contrib. Mineral. Petrol.* **78**, 452-458.

HALTER, W.E. & WILLIAMS-JONES, A.E. (1999): Application of topaz–muscovite F–OH exchange as a geothermometer. *Econ. Geol.* **94**, 1249-1258.

_____, _____ & KONTAK, D.J. (1998a): Modeling of fluid–rock interaction during greisenization at the East Kemptville tin deposit: implications for mineralization. *Chem. Geol.* **150**, 1-17.

_____, _____ & _____ (1998b): Origin and evolution of the greisenizing fluid at the East Kemptville tin deposit, Nova Scotia, Canada. *Econ. Geol.* **93**, 1026-1051.

HAM, L.J. (1991): Geological map of Windsor, Nova Scotia, NTS 21A/16 west half and part of 21H/01. *Nova Scotia Department of Mines and Energy, Map* **90–10** (1:50 000).

_____ & KONTAK, D.J. (1988): A textural and chemical study of white mica in the South Mountain Batholith, Nova Scotia: primary versus secondary origin. *Marit. Sediments Atlantic Geol.* **24**, 111-121.

HOGAN, J.P. (1996): Insights from igneous reaction space: a holistic approach to granite crystallization. *Trans. R. Soc. Edinburgh: Earth Sci.* **87**, 147-157.

HORNG, WEN-SHENG., HESS, P.C. & GAN, HAO (1999): The interactions between M^{+5} cations (Nb^{+5}, Ta^{+5}, or P^{+5}) and anhydrous haplogranite melts. *Geochim. Cosmochim. Acta* **63**, 2419-2428.

ICENHOWER, J.P. & LONDON, D. (1995): An experimental study of element partitioning among biotite, muscovite and coexisting peraluminous granitic melt at 200 MPa (H_2O). *Am. Mineral.* **80**, 1229-1251.

LONGERICH, H.P., JACKSON, S.E. & GUNTHER, D. (1996): Laser ablation inductively coupled plasma mass spectrometric transient signal data acquisition and analyte concentration calculation. *J. Anal. At. Spectrom.* **9**, 899-904.

LOWENSTERN, J.B. & SINCLAIR, W.D. (1996): Exsolved magmatic fluid and its role in the formation of comb-layered quartz at the Cretaceous Lotung W–Mo deposit, Yukon Territory, Canada. *Trans. R. Soc. Edinburgh: Earth Sci.* **87**, 291-304.

MACDONALD, M.A. (2001): Geology of the South Mountain Batholith, southwestern Nova Scotia. *N.S. Dep. Natural Resources, Open File Rep.* **ME 2001–2**.

MASSONNE, H.-J. & SCHREYER, W. (1989): Stability field of the high-pressure assemblage, talc + phengite and two new phengite barometers. *Eur. J. Mineral.* **1**, 391-410.

_____ & SZPURKA, Z. (1997): Thermodynamic properties of white micas on the basis of high-pressure experiments in the systems K_2O–MgO–Al_2O_3–SiO_2–H_2O and K_2O–FeO–Al_2O_3–SiO_2–H_2O. *Lithos* **41**, 229-250.

MCKENZIE, C.B. (1974): *Petrology of the South Mountain Batholith, Western Nova Scotia*. M.Sc. thesis, Dalhousie Univ., Halifax, N.S.

MILLER, C.F., STODDARD, E.F., BRADFISH, L.J. & DOLLASE, W.A. (1981): Composition of plutonic muscovite: genetic implications. *Can. Mineral.* **19**, 25-34.

MONIER, G. & ROBERT, J.-L. (1986a): Muscovite solid solutions in the system K_2O–MgO–FeO–Al_2O_3–SiO_2–H_2O: an experimental study at 2 kbar PH_2O and comparison with natural Li-free white micas. *Mineral. Mag.* **50**, 257-266.

_____ & _____ (1986b): Evolution of the miscibility gap between muscovite and biotite solid solutions with increasing lithium content: an experimental study in the system K_2O–Li_2O–MgO–FeO–Al_2O_3–SiO_2–H_2O–HF at 600°C, 2 kbar P_{H2O}: comparison with natural lithium micas. *Mineral. Mag.* **50**, 641-651.

MUNOZ, J.L. (1984): Fluorine index; a simple guide to high fluorine environments. *In* Micas (S.W. Bailey, ed.). *Rev. Mineral.* **13**, 469-493.

ORTOLEVA, P.J. (1994): *Geochemical Self-Organization*. Oxford University Press, Oxford, U.K.

PELRINE, K.M. (2003): *Ilmenite–Pyrophanite and Niobian Rutile in the South Mountain Batholith, Nova Scotia.* B.Sc. Honours thesis, Dalhousie Univ., Halifax, Nova Scotia.

RAIMBAULT, L. & BURNOL, L. (1998): The Richemont rhyolite dyke, Massif Central, France; a subvolcanic equivalent of rare-metal granites. *Can. Mineral.* **36**, 265-282.

RICHARDSON, J.M., BELL, K., WATKINSON, D.H. & BLENKINSOP, J. (1990): Genesis and fluid evolution of the East Kemptville greisen-hosted tin mine, southwestern Nova Scotia, Canada. *In* Ore-Bearing Granite Systems: Petrogenesis and Mineralizing Processes (H.J. Stein & J.L. Hannah, eds.). *Geol. Soc. Am., Spec. Pap.* **246**, 181-203.

RIEDER, M., CAVAZZINA, G., D'YAKONOV, Y.S., FRANK-KAMENETSKII, V.A., GOTTARDI, G., GUGGENHEIM, S., KOVAL', P.V., MÜLLER, G., NEIVA, A.M.R., RADOSLOVICH, E.W., ROBERT, J.-L., SASSI, F.P., TAKEDA, H., WEISS, Z. & WONES, D.R. (1998): Nomenclature of the micas. *Can. Mineral.* **36**, 905-912.

ROYCROFT, P.D. (1989): Zoned muscovite from the Leinster Granite, S.E. Ireland. *Mineral. Mag.* **53**, 663-665.

_____ (1991): Magmatically zoned muscovite from the peraluminous two-mica granites of the Leinster batholith, southeast Ireland. *Geology* **19**, 437-440.

SCHMITT, A.K. (2001): Gas-saturated crystallization and degassing in large-volume, crystal-rich dacitic magmas from the Altiplano-Puna, northern Chile. *J. Geophys. Res.* **106**, 30561-30578.

SPEER, J.A. (1984): Micas in igneous rocks. *In* Micas (S.W. Bailey, ed.). *Rev. Mineral.* **13**, 229-356.

TATE, M.C. & CLARKE, D.B. (1997): Compositional diversity among Late Devonian peraluminous granitoid intrusions in the Meguma Zone of Nova Scotia, Canada. *Lithos* **39**, 179-194.

TISCHENDORF, G., GOTTESMANN, B., FÖRSTER, H.-J. & TRUMBULL, R.B. (1997): On Li-bearing micas: estimating Li from electron microprobe analyses and an improved diagram for graphical representation. *Mineral. Mag.* **61**, 809-834.

VELDE, B. (1965): Phengite micas: synthesis, stability, and natural occurrence. *Am. J. Sci*. **263**, 886-913.

_____ (1980): Cell dimensions, polymorph type, and infrared spectra of synthetic white micas: the importance of ordering. *Am. Mineral.* **65**, 1277-1282.

WEBSTER, J.D. (1990): Partitioning of F between H_2O and CO_2 fluids and topaz rhyolite melt: implications for mineralizing magmatic–hydrothermal fluids in F-rich granitic systems. *Contrib. Mineral. Petrol.* **104**, 424-438.

WEIDNER, J.R. & MARTIN, R.F. (1987): Phase equilibria of a fluorine-rich leucogranite from the St. Austell pluton, Cornwall. *Geochim. Cosmochim. Acta* **51**, 1591-1597.

ZEN, E-AN (1988): Phase relations of peraluminous granitic rocks and their petrogenetic implications. *Annu. Rev. Earth Planet. Sci.* **16**, 21-51.

Received November 30, 1992, revised manuscript accepted August 4, 2003.